SIMULATION OF CHANNEL CONNECTOR BEHAVIOR USING FINITE ELEMENT METHOD

A THESIS SBMITTED TO
THE GRADUATE SCHOOL OF NATURAL AND APPLIED SCIENCES
OF
MIDDLE EAST TECHNICAL UNIVERSITY

BY

CAN AYDOĞMUŞ

IN PARTIAL FULFILLMENT OF THE REQUIREMENTS
FOR
THE DEGREE OF MASTER OF SCIENCE
IN
CIVIL ENGINEERING

AUGUST 2013

Approval of the thesis:

SIMULATION OF CHANNEL CONNECTOR BEHAVIOR USING FINITE ELEMENT METHOD

Submitted by **Can AYDOĞMUŞ** in partial fulfillment of the requirements for the degree of **Master of Science in Civil Engineering Department**, **Middle East Technical University** by,

Prof. Dr. Canan Özgen _____
Dean, Graduate School of **Natural and Applied Sciences**

Prof. Dr. Ahmet Cevdet Yalçıner _____
Head of Department, **Civil Engineering**

Prof. Dr. Cem Topkaya _____
Supervisor, **Civil Engineering Dept., METU**

Examining Committee Members:

Assoc. Prof. Dr. Afşin Sarıtaş _____
Civil Engineering Dept., METU

Prof. Dr. Cem Topkaya _____
Civil Engineering Dept., METU

Assoc. Prof. Dr. Alp Caner _____
Civil Engineering Dept., METU

Asst. Prof. Dr. Eray Baran _____
Civil Engineering Dept., Atılım University

Dr. Cenk Tort _____
Director (Research and Development), MİTENG

Date: August 15th, 2013

I hereby declare that all information in this document has been obtained and presented in accordance with academic rules and ethical conduct. I also declare that, as required by these rules and conduct, I have fully cited and referenced all material and results that are not original to this work.

Name, Last Name : Can, Aydoğmuş
Signature :

ABSTRACT

SIMULATION OF CHANNEL CONNECTOR BEHAVIOR USING FINITE ELEMENT METHOD

Aydoğmuş, Can
M.S., Department of Civil Engineering
Supervisor: Prof. Dr. Cem Topkaya

August, 2013, 73 pages

Channel shear connectors are fairly new alternatives to the shear connectors. In this thesis two of the previously done experimental studies were simulated using FEM. First, push-out tests consisted of ten specimens which include European channel sections as shear connectors were modeled in ANSYS. The models with simplistic materials and 2D elements were analyzed. Analysis results were compared with the experimental results. Comparisons showed that, 2D models with bilinear materials were sufficient enough to provide practical ultimate capacity predictions. Second, full-scale beam test with channel shear connectors were simulated. Experiments included four specimens with differentiating connector numbers. The general aim was to investigate the partial and full composite action. 3D FE models were created with several concrete modeling approaches and difficulties in modeling were mentioned. One stable concrete model was found and selected for use. Experimental results and analysis result were compared. Also comments were made on model behavior. In conclusion, FE modeling details were reviewed and criticized.

Keywords: Composite Beam, Channel Shear Connector, Finite Element Method, ANSYS, Concrete Material Modeling

ÖZ

SONLU ELEMANLAR METODU KULLANILARAK U-PROFİL BAĞLANTI ELEMANLARININ SİMÜLE EDİLMESİ

Aydoğmuş, Can
Yüksek Lisans, İnşaat Mühendisliği Bölümü
Tez Yöneticisi: Prof. Dr. Cem Topkaya

Ağustos, 2013, 73 sayfa

U-Profil bağlantı elemanları kesme bağlantıları içerisinde epey yeni bir alternatiftir. Bu tezde daha önceden yapılmış olan iki deney çalışması sonlu elemanlar metodu kullanılarak simüle edilmiştir. İlk olarak, Avrupa standardı u-profillerini kesme elemanı olarak kullanan 10 deney numunesi ANSYS' de modellenmiştir. Basitleştirilmiş malzemeler ve 2 boyutlu elemanlar kullanılan modeller analiz edilmiştir. Analiz sonuçları deney sonuçlarıyla karşılaştırılmıştır. Karşılaştırma göstermiştir ki, bilineer malzemeler kullanılmış 2 boyutlu modeller de pratik kapasite tahminleri verecek kadar etkili çalışmaktadır. İkinci olarak, u-profilleri bağlantı elemanı olarak kullanan gerçek ölçekli kiriş testleri simüle edilmiştir. Deneyler farklı sayıda bağlantı elemanı kullanan dört numuneden oluşmaktadır. Genel amaç kısmi ve tam kompozit etkinin incelenmesidir. Birçok farklı malzeme modelinin denendiği 3 boyutlu model oluşturulmuş ve modelleme sırasında oluşan problemlere değinilmiştir. İçlerinden istikrarlı olan bir beton modeli kullanmak üzere seçilmiştir. Deney ve analiz sonuçları karşılaştırılmıştır. Ayrıca modellerin davranışları üzerine yorumlarda bulunulmuştur. Sonuç olarak sonlu eleman modellemenin detayları incelenmiş ve eleştirilmiştir.

Anahtar Kelimeler: Kompozit Kiriş, U-Profil Kesme Bağlantısı, Sonlu Eleman Metodu, ANSYS, Beton Malzeme Modeli

ACKNOWLEDGEMENTS

The partial found for this thesis has been supplied by the TUBİTAK under grant number 212M038. Financial support is gratefully acknowledged.

I would like to thank to my supervisor, Prof. Dr. Cem Topkaya, for taking a chance on me and supporting me through these years. This thesis would not have been possible without his tolerance. Also, I would like to thank to Asst. Prof. Dr. Eray Baran for his guidance and financial supports. To both of them, I am indebted and can only express my sincere appreciation.

I thank all my professors at METU for tolerating my endless questions and for their sincere supports. Furthermore, I thank all my professors at Eskişehir Osmangazi University for grooming me to a better future. Thank you for mentoring me.

Lastly, to my parents and my dear sister, thank you for being with me in this long journey.

TABLE OF CONTENTS

APPENDIX

LIST OF TABLES

TABLES

LIST OF FIGURES

FIGURES

CHAPTER 1

INTRODUCTION

1.1 Composite Action

Composite members in which reinforced concrete decks positioned on steel girders are being used for a considerable time in bridge and building construction. When steel and reinforced concrete are used separately they present some shortcomings and those shortcomings may increase the cost of the construction. For example, steel girders are fabricated using thin plates and as a result of that they are prone to local and lateral buckling as well as fatigue (Oehlers and Bradford, 1995). Also, the concrete sections are generally thick and unlikely to buckle. However, unlike their high strength in compression they present weak behavior when they are subjected to tension. Despite these problems combining steel and concrete in right combination which uses each other's positive attributes brings advantages to both elements.

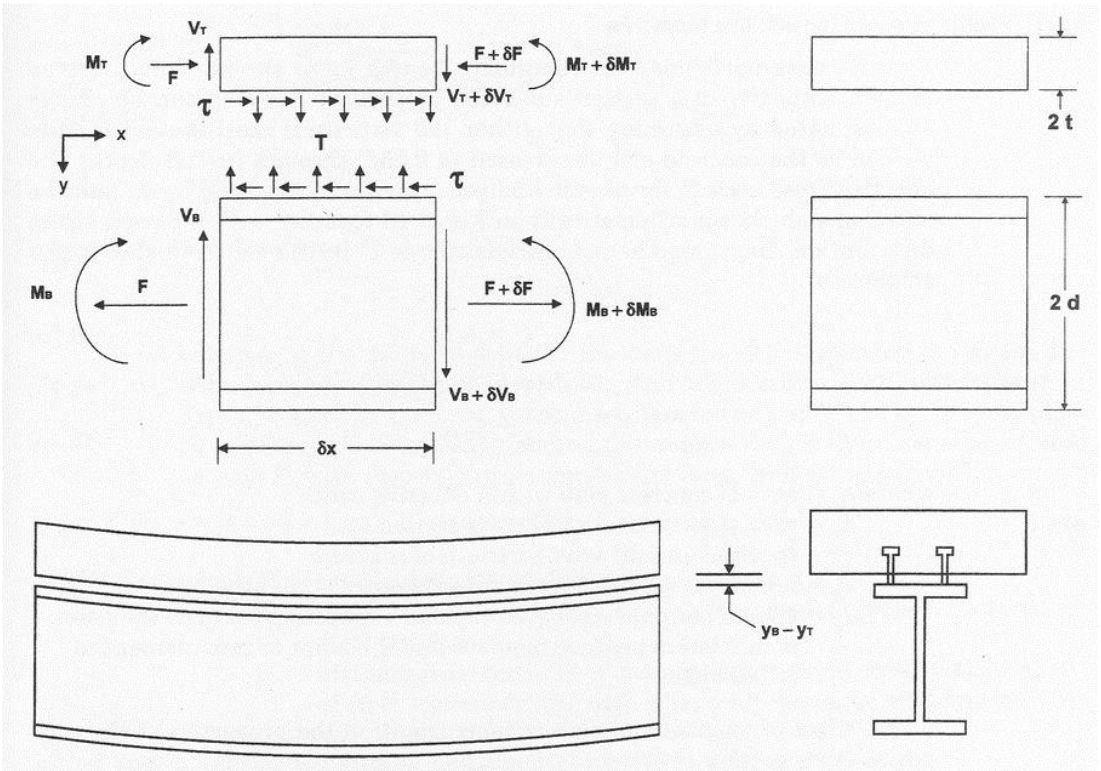

Figure 1.1 Forces Acting on a Composite Section (Ref: Viest et al., 1997)

Composite beams are generally assumed to be loaded in flexure (Fig.1.1). This creates such a condition that steel girder works in tension and the reinforced concrete deck works in compression.

This working condition can only be made possible if two elements steel girder and reinforced concrete deck are connected intermittently so that they can work as one. To transfer the horizontal shear force between the steel girder and the reinforced concrete deck interface several mechanisms can be utilized such as adhesion, friction and bearing (Viest et al., 1997).

In most composite beams shear connection is provided using a steel member welded to the top flange of the steel girder and embedded in reinforced concrete. Those members transfer the forces between steel girder and the connector by shear and between connector and concrete by bearing (Viest et al., 1997).

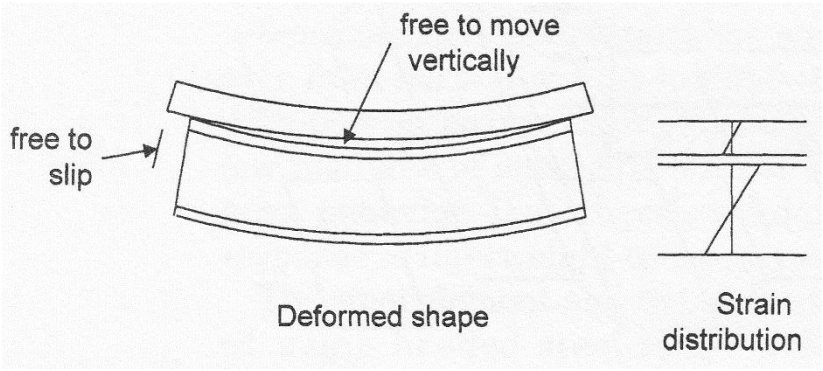

Figure 1.2 No Interaction (Ref: Viest et al., 1997)

The connection provided between the steel girder and the reinforced concrete deck is important. If we assume that there is no connection between two mediums; the applied flexural forces would be resisted by steel girder and concrete deck separately (Fig.1.2). Despite the sound and the fire insulation this combination would not be satisfactory.

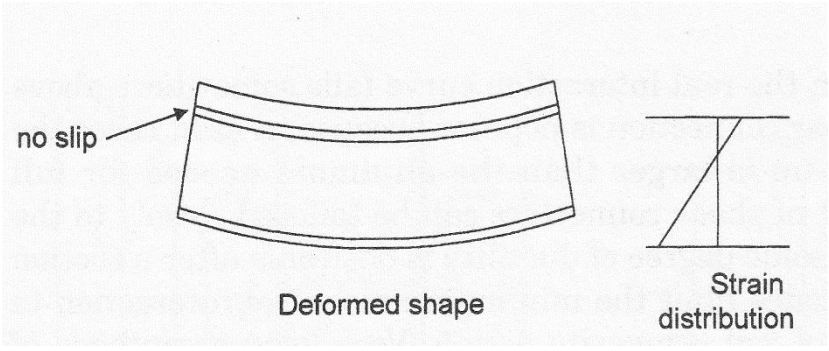

Figure 1.3 Complete Interaction (Ref: Viest et al., 1997)

In the most satisfactory case steel girder and the reinforced concrete deck would be connected and react as one member (Fig.1.3). Under flexural loading, concrete is weak in tension so steel girder would provide the necessary tensile strength and with a minimum section depth concrete would carry the compression. The depth of the beam subjected to the flexure is now increased from that of the girder acting by itself so this would increase the flexural strength and stiffness of the section resulting in a decrease in section height and cost, making composite sections more economical and more efficient from other options.

1.2 Shear Connection

Shear connection between steel girder and reinforced concrete deck is the key element for successful composite action. To be able to calculate the strength of the composite beam, designers should understand the quantitative behavior and the strength of the shear connectors.

To this day various shear connectors has been used and tested, but without any question welded headed shear stud (Fig.1.4) is the most common connector today.

Figure 1.4 Headed Shear Stud (Ref: directindustry.com, June, 2013)

The body of the stud and the weld are designed to resist the longitudinal shear forces while the head is designed to resist the tensile loads that are perpendicular to the shear forces between the steel and the concrete interface as it is shown in Fig.1.1.

Every shear connector including the headed shear stud is designed according to two fundamental principles. First, they must resist the horizontal shear forces developed at the interface between two mediums. Second, they should not let the pull up forces to separate the two mediums by resisting the tension forces. There is a large variety of mechanical shear connectors, varying in shape, size and methods of attachment (Fig.1.5). However, they all have the following similarities;

- All mechanical shear connectors are dowels embedded in concrete.
- They have one component to resist the horizontal shear forces and one other component that resists the tensile forces perpendicular to the shear forces hence preventing separation of the two mediums (Oehlers and Bradford, 1995).

Push-out tests are the most common ways to provide an insight to the behavior and strength of the headed shear stud. Although the test has been developed in 1930's (Viest et al., 1997) there is no generally accepted or standardized procedure.

Researchers have been using couple of different test methods but results typically consist of Load vs. Slip relationship and failure mode.

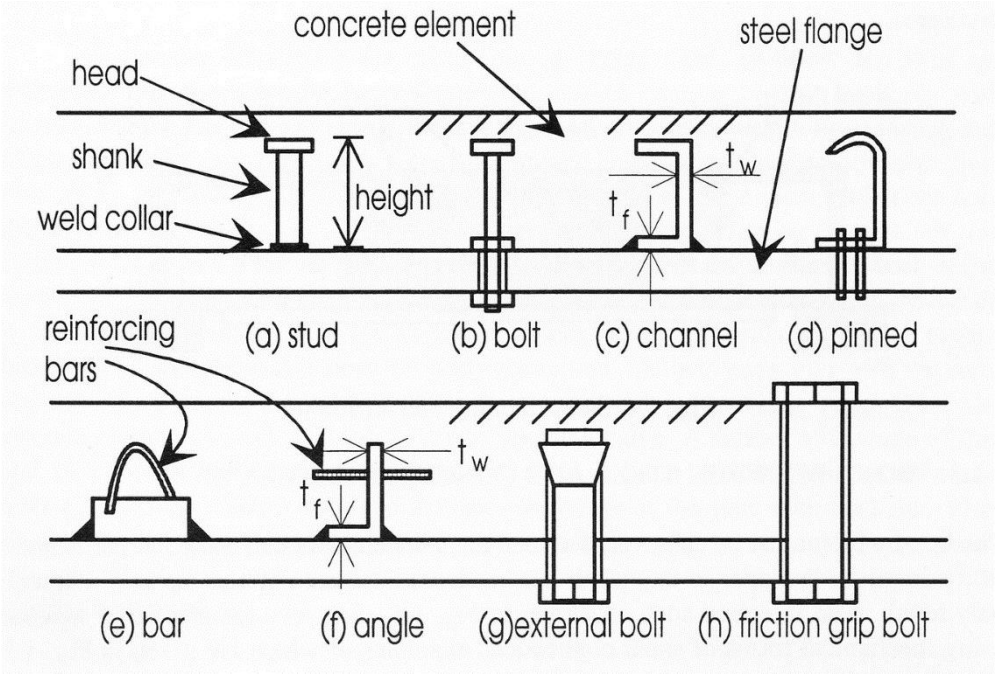

Figure 1.5 Mechanical shear Connectors (Ref: Oehlers and Bradford, 1995)

Most common push-out specimens are very similar to those which have been tested at Lehigh University by Olgaard et al. (1971) as shown in Fig.1.6. However, there is a problem associated with this method. The concrete blocks had to be cast on two different days resulting varying concrete strengths in specimen. Several alternative methods have been generated by researchers to solve this problem.

According to the test procedure, specimens are placed on a universal testing machine on two bearing pads to eliminate the uneven geometry and minimize its effects. Shear load is applied gradually using the machine with increments that are approximately 10 percent of the expected specimen capacity. During the test, amount of slip vs. applied load is recorded.

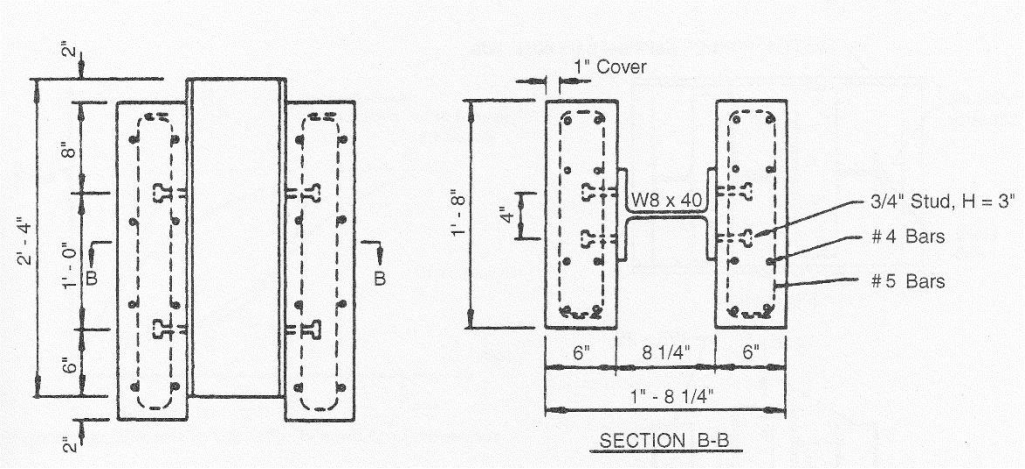

Figure 1.6 Typical Push-Out Test Sipecimen (Ref: Viest et al., 1997)

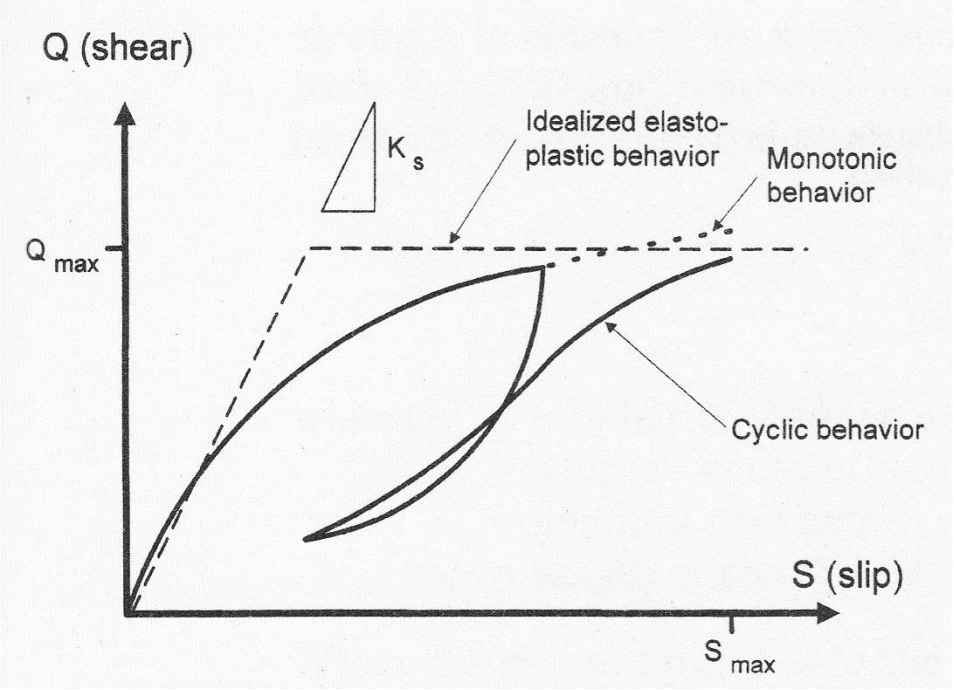

Figure 1.7 Typical Push-Out Test Sipecimen (Ref: Viest et al., 1997)

Generally results will show similarity to Fig.1.7. These tests are usually run monotonically, the figure also shows the unloading behavior after significant slip has occurred in case of a major overload event (Viest et al., 1997).

1.3 Channel Shear Connectors

Popular use of headed shear connectors comes from their proven performance and easy application process using a welding gun. Even though headed shear studs are popular, their

application and installation comes with reliability problems. Unless true care is given to the installation process, welding strength and performance can be affected substantially by the weather, coating material of the steel and surface conditions (Chien and Ritchie, 1984).

Because of their small load capacity, headed shear connectors are needed to be installed in large amounts. This creates a crowded and unsafe working place. Due to these entire drawbacks, researchers and construction companies headed toward the pursuit of other better performing shear connectors.

Channel shear connectors are one of the tried mechanical connectors and in many aspects which are listed below they are exceeding the headed studs' performance;

- While studs need special equipment like welding guns, conventional welding equipment is enough for channel shear connectors.
- By contrast conventional welding has a proven performance and it is more reliable than welding used to install the headed studs.
- Channel shear connector's load carrying capacity is at least 2 times greater than the headed shear studs, in some cases more, and this result in fewer shear connectors.
- Fewer shear connectors means a substantial decrease in work time.
- Conventional welding and channel connectors are more robust and can tolerate rough handling.
- Using channel connectors with fewer elements creates safer work environment.

Figure 1.8 Headed Stud Shear Connector Clutter
(Ref: steelconstruction.info, June, 2013)

All of these aspects make a good case for channel shear connectors. However, there is not much research done to understand the behavior and the performance of channel shear connectors. The reason for the lack of study may be the popularity of the headed studs. There are already excessive amount of research for headed studs. Furthermore, figuring out one connector's behavior means lots of research and numerical analyses and all those cost money. There are a couple of published research which take subject to understand the channel connectors' behavior by performing push-out and full scale beam tests.

Some of this research is mentioned in following sections.

1.4 Illinois Bulletin (Viest et al., 1952)

Regarding couple of previous research authors present couple of unanswered questions. After some prior testing (Siess, 1949, Siess et al., 1952) it was concluded that more detailed push-out testing can give more satisfactory answers towards performance of the channel shear connectors and their behavior in composite beams.

Primary objective was to investigate the behavior of channel connectors used in composite beams.

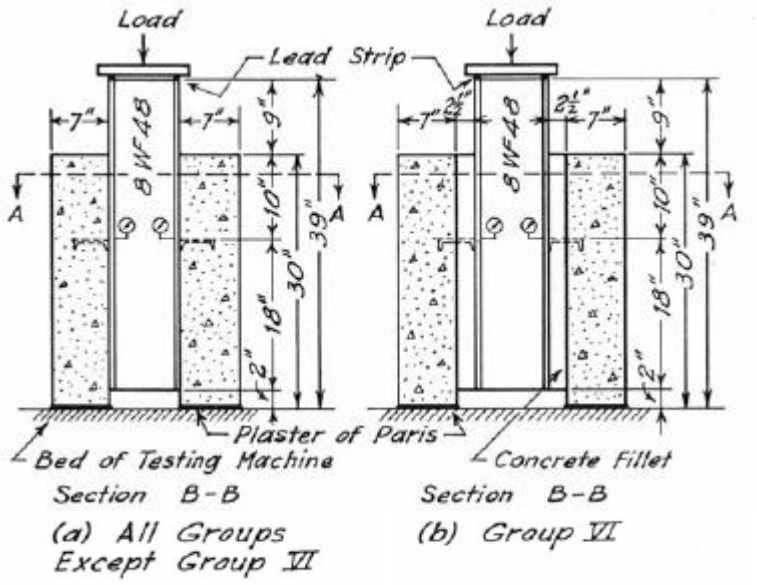

Figure 1.9 Push-Out Specimens (Ref: Viest et al., 1952)

In total forty-three push-out specimens (Fig.1.9) divided in seven groups were tested. Principle variables were strength of concrete, dimensions of channel shear connectors, the restraint of concrete under the connector and the direction of load. These tests were designed to provide;

1. Information about the behavior of channel shear connectors.

2. Insight for effects of the mentioned variables on channel connector's behavior and load carrying capacity.

Summary of the mentioned seven groups are listed in Table 1.1.

Throughout the research it can clearly be seen that most of the specimens included 4in (102mm) height channel connectors. There were only two specimens that included 5in. (127 mm) connectors and three specimens with 3in. (76mm) connectors.

Tests results showed that flange thickness, web thickness and length of the connector, had affected the behavior of the channel significantly. The orientation of load whether channel loaded from its back or front side did not make any mentionable effect on connector's behavior.

Table 1.1 Push-Out Specimens of Viest et al. (1952)

Group	Number of Specimens	Parameters	f'c	Connectors
1	11	Strength of Concrete	14.27 - 43.57MPa (2070 - 6320psi)	4 in. (102mm) 5.4 lb
2	10	Connectors Web Thickness	15.86 - 34.50MPa (2300 - 5000psi)	4 in. (102mm) 7.25 lb 4 in. (102mm) 7.25 lb 4 in. (102mm) 13.8 lb
3	6	Connectors Flange Thickness	13.80 - 23.45MPa (2000 - 3400psi)	4 in. (102mm) 5.4 lb 4 in. (102mm) 7.25 lb 4 in. (102mm) 5.4 lb + 0.5 in. plate 4 in. x 0.5 in. plate 1.25 in. x 1.25 in. plate 1 in. x 1 in. Plate
4	5	Connector Height	20.70 - 27.60MPa (3000 - 4000psi)	3 in. (76.2mm) 4.1 lb 5 in. (127mm) 6.7 lb
5	2	Connector Width	19.30 - 30.50MPa (2800 - 4400psi)	4 in. (102mm) 5.4 lb 4 in. (102mm) 5.4 lb
6	7	Restraint of Concrete Under Connector	15.20 - 32.40MPa (2200 - 4700psi)	4 in. (102mm) 5.4 lb 4 in. (102mm) 5.4 lb 4 in. (102mm) 7.25 lb 1 in. x 1 in. Plate
7	2	Direction of Load	~20.70MPa (3000psi)	4 in. (102mm) 5.4 lb

As discussed in the report, data taken from 8 specimens were unreliable because of the experimental problems faced during the tests. Additionally, the number of specimens was found inadequate in each individual parameter.

As a result, researchers were not able to present or develop any reliable equation for predicting the capacity of channel shear connectors embedded in solid concrete slabs. Although the research provided significant insight towards the behavior of channel shear connectors and contributions of mentioned parameters to the channel connector capacity, there was a need for detailed research.

1.5 Work of Slutter and Driscoll (1965)

This study was part of an investigation on ultimate strength capacities of composite steel and concrete beams. Throughout the study various types of mechanical shear connectors were tested and one of them was channel shear connector. The aim was to develop a criterion for minimum shear connector requirements for composite beams.

In 1957 for the revision of ASSHO, semi empirical equations for useful capacity of various mechanical shear connectors were developed. After this in 1960, ASCE-ACI committee for composite construction retained the ASSHO equations but added a factor of safety for statically loaded members. These equations were satisfactory for structural safety perspective however these do not provide economical solutions.

Experimental program included;

- 12 simple span composite beams with 15ft (4.57m) span
- One two-span continuous composite beam with also 15ft (4.57m) spans
- Also, nine push-out specimens.

All beams consisted of one 12WF27 steel girder and a concrete deck with 4in. (101.6mm) thickness and 4ft. (1220mm) width. Only two of the beams were designed with natural bond but other beams had shear connectors welded to their flanges. One of the thirteen beams consisted of channel shear connectors others had bent and headed shear studs.

After the tests researchers generated an equation for estimating the ultimate load capacity of one channel connector.

$$q_u = 550.(h + 0.5t)w\sqrt{f_c'} \qquad \text{(Eq.1.1)}$$

where;
h : average flange thickness of the channel (in.)
t : web thickness of the channel (in.)
w : length of the channel (in.)
f'_c : compressive cylinder strength of concrete (psi)

According to the researchers this equation gives more economical estimates than equations in AISC-1961.

1.6 M.Sc. Thesis by Amit Pashan (Pashan, 2006)

Even after several years from the original attempts to use channel sections as shear connectors in composite beams there were still not enough research that defines the behavior of channel shear connectors as accurate as the headed shear connector.

The test program tried to answer couple of questions unanswered by the previous researchers by increasing the specimen number and changing the parameters. By doing so, the author intended to develop new equations that are more inclusive for channel shear connectors embedded in;

1. Solid concrete slabs,
2. Slabs with wide ribbed metal deck oriented parallel to the beam.

Test specimens were designed to study several parameters. The main parameter was the channel height and the other parameters were compressive strength of the concrete, length and web thickness of the channel.

In total 78 push-out specimens were tested in two phases divided in six series. A summary for the experimental program is shown in Table 1.2.

Table 1.2 Push-Out Specimens of Pashan (2006)

Phase 1

Series	Slab Type	Number of Specimens	Channel Height	Parameters	
A	Solid	12	127 mm	Channel Length Web Thickness	Compressive Strength of Concrete
B	Solid + Deck	6 + 6		Channel Length Web Thickness	
C	Solid + Deck	6 + 6		Channel Length Web Thickness	
Total		*36*			

Phase 2

Series	Slab Type	Number of Specimens	Channel Height	Parameters	
D	Solid + Deck	6 + 6	102 mm	Channel Length Web Thickness	Compressive Strength of Concrete
E	Solid + Deck	6 + 6		Channel Length Web Thickness	
F	Solid + Deck	6 + 6		Channel Length Web Thickness	
Total		*36*			

Results showed that increase in channel length increased the channel shear connector capacity almost linearly. When the channel length increased from 50mm to 100mm the capacity increased by 39%. Capacity increased further by 24% when the channel length increased from 100mm to 150mm. Changes in channel web thickness had a significant impact on failure due to channel fracture. Nevertheless web thickness did not affected failure by concrete crushing and splitting so much.

It was found out that solid concrete slabs had higher load capacities than metal deck slabs because of the high concentrated loads in relatively small areas. Increase in load capacity was 12% for specimens with 50mm long channels on the other hand for specimens with 150mm long channel connector load capacity increased by 33%.

Based on these results researchers developed two new equations that predicts the ultimate load carrying capacity for both shear connectors embedded in solid slabs and wide ribbed metal decked slabs.

Even though these test result are deemed reliable and successful, specimen selection and test assembly brings some challenges. Channel length varies by 50-100-150mm this seems viable though channel height represents ones in 102mm to 127mm range. Also, channels with only two web thicknesses were used 4.7 and 8.2mm.

As a result, equation developed by Pashan represents the channel heights between 102 to 127mm. The performance of the equation was discussed and the drawbacks were laid out in the next sections.

1.7 Works of Maleki and Bagheri (2008)

This research studied the behavior and the effects of different concrete materials. In total 16 push-out specimens were prepared using plain concrete (C), reinforced concrete (RC), fiber reinforced concrete (FRC) and engineered cementitious composite (ECC).

Three parameters were selected to serve the main purpose; type of loading (monotonic and low-cycle fatigue loading), length of the channel (30 and 50 mm), concrete materials and reinforcement (FRC, ECC, and with or without reinforcement). Within these 16 push-out specimens 9 of them were tested under monotonic loading other 7 were tested under fully-reversed low cycle loading.

After tests two failure modes were observed;

1. Channel fracture – fracture of the channel web near bottom flange
2. Concrete crushing and splitting

Summarized version of the push-out specimens with variables and failure modes are given in Table 1.3.

Results showed that monotonic shear strength capacities of specimens were 10 to 23% higher than the reversed cyclic shear strengths. FRC had a slight effect on shear strength, although ECC caused considerable increase in ultimate strength and ductility.

Table 1.3 Push-Out Specimens of Maleki and Bagheri (2008)

Specimen	Loading	Channel Length	Reinforcement	Failure Mode
C -1	M	50 mm	No	Mode #2
C - 2	C			Mode #2
RC - 1	M	50 mm	Yes	Mode #1
RC - 2	C			Mode #1
RC - 3	M	30 mm	Yes	Mode #1
RC - 4	C			Mode #1
FRC - 1	M	50 mm	No	Mode #2
FRC - 2	C			Mode #2
FRC - 3	M	30 mm	No	Mode #2
FRC - 4	M	50 mm	Yes	Mode #1
FRC - 5	C			Mode #1
ECC - 1	M	50 mm	No	Mode #2
ECC - 2	C			Mode #1
ECC - 3	M	30 mm	No	Mode #1
ECC - 4	C			Mode #1
ECC - 5	M	50 mm	Yes	Mode #1

*M for monotonic loading
*C for cyclic loading
Mode #1 : Channel Fracture
Mode #2 : Conc. Crushing & Splitting

In the second part of the research, focus was on the channel shear connector embedded in solid concrete slab and under monotonic loading. The main objective was to develop three dimensional finite element models using the commercially available program called ANSYS, and also to simulate the behavior of channel shear connectors.

As a finite element model, concrete and steel elements were modeled using 8-node elements in ANSYS (Table 1.4).

Effect of steel beam was insignificant in push-out tests so it was not modeled and the load was applied to the lower flange of the channel connector.

Steel was modeled bilinear using the material data supplied in part one of the research. However, concrete material was modeled using a special model called Cast Iron Plasticity. This model was almost never used to model concrete like materials but authors reflected that it was used to utilize the different tension and compression capacities of concrete.

Table 1.4 Elements Used in Maleki and Bagheri (2008)

Elements in Push-Out Test Setup	Elements Used in ANSYS
Steel Channel	SOLID45
Concrete Deck	SOLID185
Interaction Between	CONTAC52

Keeping in mind the nonlinearity load was applied as displacement, and it was applied to the bottom flange of the connector. To solve the nonlinear problems ANSYS employs various approaches, in this case researcher used Newton-Raphson Method. This method uses several substeps to apply the load (displacement) gradually.

Results showed a good correlation in load and displacement curves between FE and the experiment. Model was verified against experimental test results and after that parametric study was conducted to evaluate the effects of compressive strength of concrete, channel dimensions and orientation.

As a result, research reflected that there were significant relationships between ultimate load capacity and compressive strength of concrete, web thickness, flange thickness and length of the channel although height of the channel had no significance. Additionally, changing the orientation of the channel connector changed the stiffness and ultimate strength.

1.8 Experimental Study by Baran and Topkaya (2012)

There are still some questions about channel shear connectors, and researchers are trying to answer them. Though it has been approximately sixty years since Viest et al. (1952), improvements toward channel shear connectors are developing in a slow pace.

Equations given by standards (CSA, 2001 and AISC, 2005) and generated by other researchers (Pashan, 2006) for estimating a channel connectors' ultimate load capacity were derived using limited sample ranges. This causes serious challenges with out of range channel connectors. Also, most of the previous research was consisted of North American channel connectors. European channel sections are different form their North American counter parts, hence the questions are: What is the ultimate capacity of specimens that are configured with European channel sections and how do they behave.

This section includes detailed information and test methodology of an experimental program done by Baran and Topkaya (2012) which consisted of push-out specimens with commercially available European channel sections as shear connectors embedded in solid concrete slab.

When it comes to conventional push-out tests there are a couple of problems and they have been mentioned briefly. Conventional push-out specimens are prepared with two concrete solid slabs on each flange of a girder so each side of the specimens needs to be cast on different times. This causes two solid concrete slabs with different compressive strengths. It

is a well-known fact that concrete strength is an important factor for ultimate connector capacity. Having two separate concrete slabs with different compressive strengths interrupts the purpose. Also it would cause uneven load and stress distribution.

Push-out specimens and the test assembly mentioned in this study was prepared as an alternative for conventional push-out tests and is an updated version of what was used in Topkaya (2004).

For testing push-out specimens with early age concrete Topkaya (2004) proposed a new test setup. Tests included specimens with early age concrete from 3 to 48 hours after casting concrete to be subjected to shear forces. Thus some changes needed to be made; tests should be completed in short time, when testing finished, specimens are not to be removed which rules out the universal testing machines used in previous push-out tests, and finally specimens were not to be anchored to the floor or another surface. As a result a self-confined test setup was developed as shown in Fig.1.10.

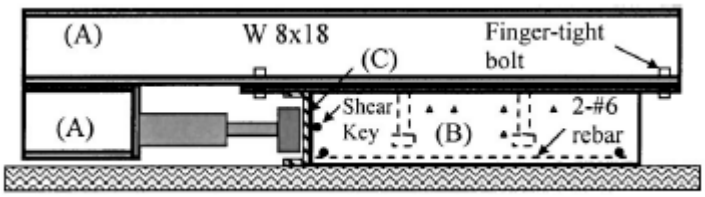

Figure 1.10 Push-Out Test Setup (Ref: Topkaya, 2004)

The situation in mentioned research was not present for this experimental program however it was decided to adopt the proposed test setup and change it to make a good use of the advantages it brings.

1.8.1 Introduction to the Experimental Program

Experimental program includes ten push-out specimens with channel shear connectors embedded in solid concrete slab. Testing was done in two parts each with five push-out specimens.

Case 1 involved five push-out specimens with solid concrete slabs as mentioned earlier. Specimens in this case were consisted of commercially available European channel sections as shear connectors. All specimens of this case featured 50mm long channels. Just as same as the Case 1, five push-out specimens were included in Case 2. The only difference between the cases was channel lengths. This case featured 75mm long channels.

Necessary tests were done by a team in Atılım University Structural Mechanics Laboratory with the supervision of Baran and Topkaya.

1.8.2 Program

As mentioned before in the previous researches steel girder in the push-out specimen had no influence besides transferring the applied load from the universal testing machine as shear force to the channel shear connectors. For this reason the steel girder is eliminated and replaced/represented by a rigid steel plate. Additionally steel base plate was provided with four holes to help the anchoring.

Channel connectors with different heights and lengths were welded to this plate. To prevent the specimen from moving this plate is constrained to the test setup. For all specimens slab thickness was 18cm additionally overall specimen was 50cm wide and 70cm long as shown in Fig.1.11.

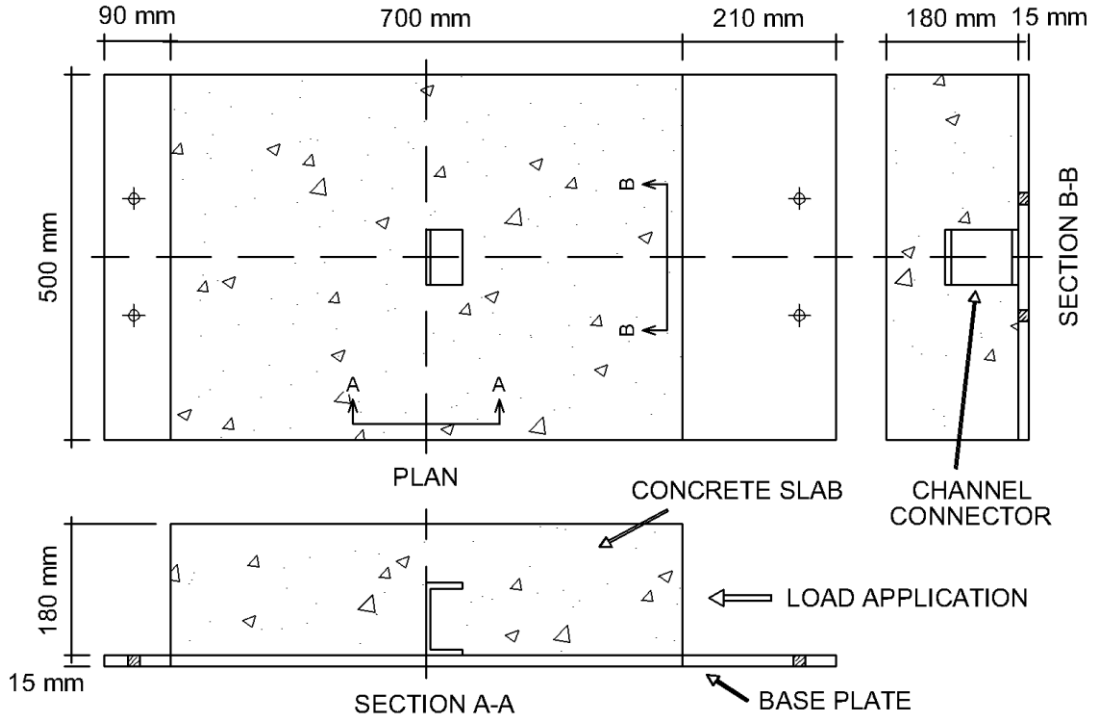

Figure 1.11 Push-Out Specimen

Channel connectors were positioned right in the middle of the specimen and welded directly to the base plate.

Longitudinal reinforcements in all specimens were consisted of eight, 10mm diameter steel bars spaced at approximately 15cm, four on the bottom and four on top. Transverse reinforcements were consisted of ten, 10mm diameter steel bars divided equally for bottom and top also they were spaced at 14cm. Bottom reinforcements were placed roughly 2.5cm from the base plate. Reinforced specimen drawing can be seen in Fig.1.12.

After channel connectors were welded to the base plate reinforcements were placed and specimen was ready for concrete (Fig.1.14). Concrete mixture was prepared on the facility using a concrete mixer. When casting the concrete three, 15cm diameter to 30cm long

concrete cylinders were prepared for each specimen as shown in Fig.1.13. Before testing cylinders and push-out specimens were cured in necessary conditions for 28 days in the facility where they were prepared.

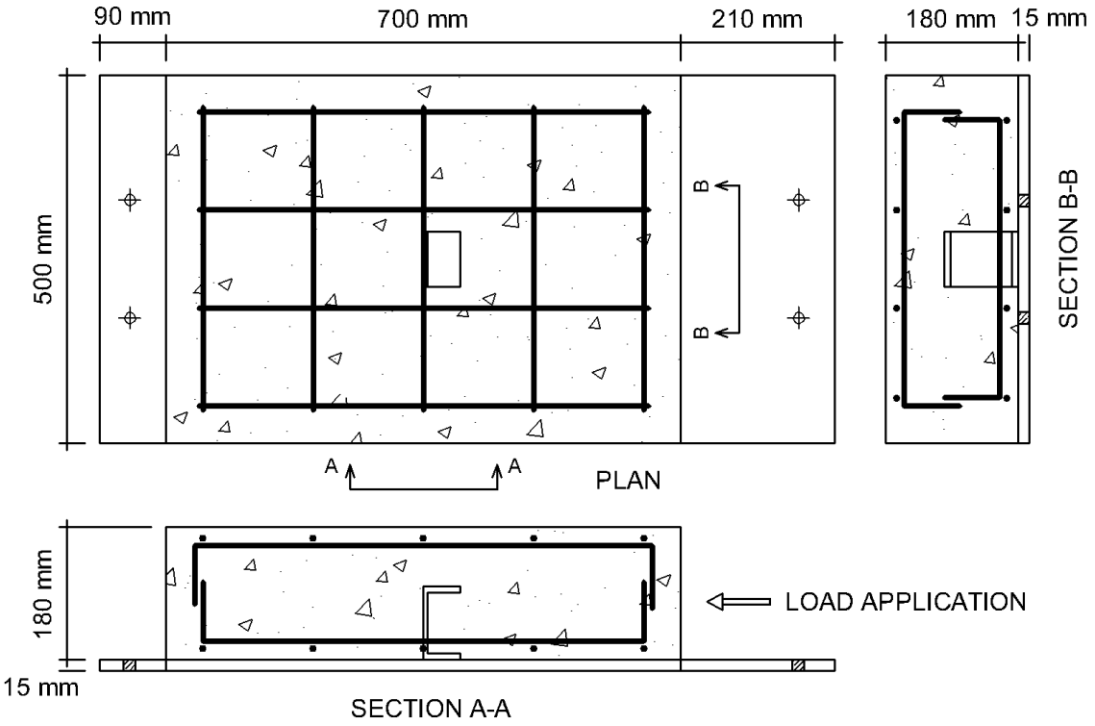

Figure 1.12 Push-Out Specimen Reinforcement Drawing

Specimens in Case 1

The main testing parameter for Case 1 was the channel height. Every channel section used for testing was selected from commercially available European sections. Sections U65, U80, U100, U120, and U140 were the channel shear connectors that were embedded in the solid concrete slab. Length of the channels for this case was set to 50mm.

Specimens in Case 2

This case was produced to understand the relationship between ultimate load carrying capacity of channel shear connectors and length of the channel. Therefore every specimen in this case had 75mm long channel connectors. There were five specimens each with different channel height.

Differences within cases would show the relationship between ultimate load capacity and channel height whereas differences between cases would reflect the relationship between ultimate load capacity and channel length.

Properties of channel shear connectors and a summary of the experimental study is presented in Table 1.5 and Table 1.6, respectively.

Figure 1.13 Push-Out Specimen and Cylinders

Table 1.5 Geometric Properties of Channel Sections

Section	Channel Sections			
	Height, H (mm)	Flange Width, W (mm)	Web Thickness, tw (mm)	Flange Thickness, tf (mm)
UPN 65	65	42	5.5	7.5
UPN 80	80	45	6	8
UPN 100	100	50	6	8.5
UPN 120	120	55	7	9
UPN 140	140	60	7	10

1.8.3 Test Setup

Specimen that cured for at least 28 days was placed on the setup and fastened from the base plate to the assembly. Due to an experience from preliminary tests, specimen was fastened to the assembly from its top using a steel member and to eliminate the friction between concrete slab surface and the steel member a Teflon sheet is placed beneath it.

This last addition to the test setup was made to resist the uplift effect caused by the interaction between channel connector and concrete. After steel connector starts to yield channel behaves like a cantilever with larger displacements thus the upper flange of the channel starts to lift the concrete slab up when it deforms.

Table 1.6 Push-Out Specimen Details of Experimental Study by Baran and Topkaya (2012)

	Specimens	Channel Sections	Parameters Height (mm)	Parameters Length (mm)	Concrete Strength (MPa)
Case 1	U65 - 50mm	UPN65	65	50	31.8
	U80 - 50mm	UPN80	80	50	33.3
	U100 - 50mm	UPN100	100	50	32.2
	U120 - 50mm	UPN120	120	50	39.9
	U140 - 50mm	UPN140	140	50	36.7
	-	-	-	-	-
Case 2	U65 - 75mm	UPN65	65	75	34.7
	U80 - 75mm	UPN80	80	75	33.8
	U100 - 75mm	UPN100	100	75	35.4
	U120 - 75mm	UPN120	120	75	32.7
	U140 - 75mm	UPN140	140	75	32.9

Two LVDT displacement transducers were installed at the opposite end of the specimen (Fig.1.15) from where the load applied, to measure the displacement of concrete slab. When the load is applied from the right hand side of the specimen concrete slab will displace and the transducers will collect the data.

Lastly, a distributing plate was placed between the specimen and the loading head of the testing machine. Displacement readings were monitored and recorded through a data acquisition system connected to the displacement transducers.

All specimens were tested under monotonic loading just like the conventional push-out tests. Load is applied incrementally with time using a hydraulic cylinder which a load cell placed in front and data acquisition system recorded the applied load in time. Test was continued and load was applied until a sudden failure like channel fracture failure as shown in Fig.1.16.

Detailed information about the experiment and results can be found in Baran and Topkaya (2012).

Figure 1.14 Push-Out Specimen with Reinforcement

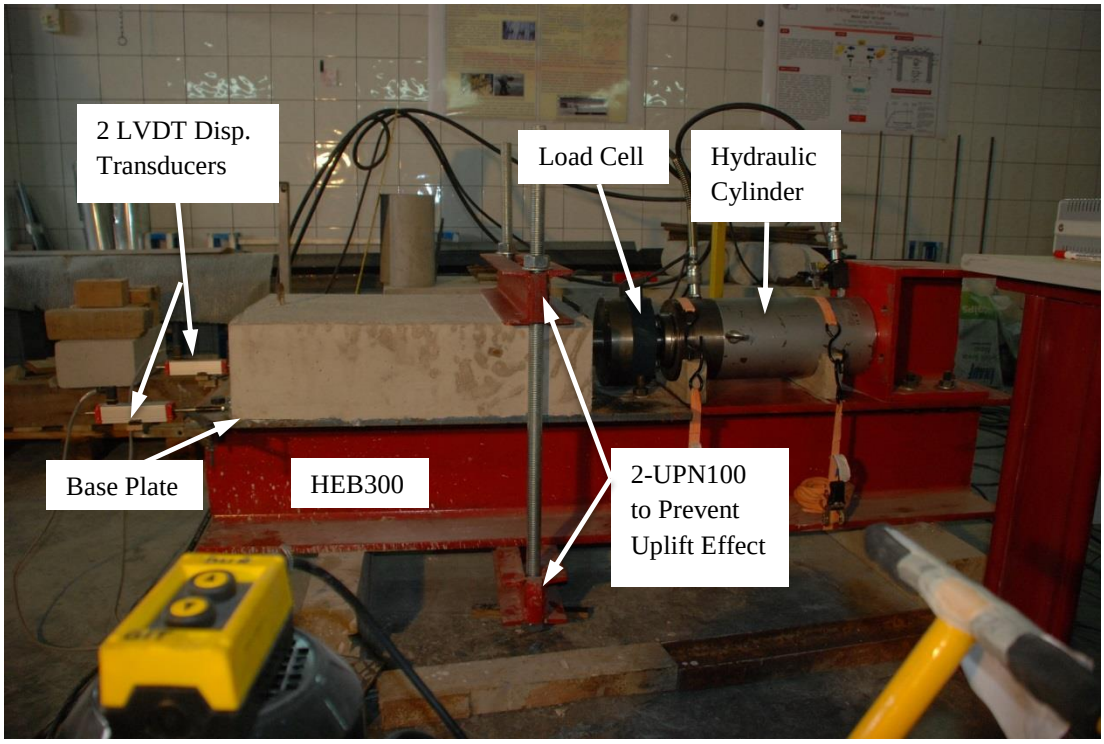

Figure 1.15 Test Setup

1.8.4 Material Properties

The three cylinder concrete samples for each specimen were tested with push-out specimens. Average values of three associated cylinders were taken as the compressive strength of the concrete used in that specific push-out specimen. Compressive strength values of push-out specimens varied from 31.8 to 39.9 MPa as it is shown in Table.1.7.

Table 1.7 Cylinder Compressive Strengths of Push-Out Specimens

	Specimens	Cylinder #1	Cylinder #2	Cylinder #3	Avrg. Comp. Strength
Case 1	U65 x 50mm	31.6 MPa	33.3 MPa	30.6 MPa	**31.8 MPa**
	U80 x 50mm	33.1 MPa	32.7 MPa	34.0 MPa	**33.3 MPa**
	U100 x 50mm	32.7 MPa	31.5 MPa	32.4 MPa	**32.2 MPa**
	U120 x 50mm	40.1 MPa	39.6 MPa		**39.9 MPa**
	U140 x 50mm	37.3 MPa	35.8 MPa	37.1 MPa	**36.7 MPa**
	-	-	-	-	-
Case 2	U65 x 75mm	34.8 MPa	34.6 MPa	34.5 MPa	**34.6 MPa**
	U80 x 75mm	32.3 MPa	34.9 MPa	34.2 MPa	**33.8 MPa**
	U100 x 75mm	34.8 MPa	35.5 MPa	35.8 MPa	**35.4 MPa**
	U120 x 75mm	32.9 MPa	32.5 MPa	32.7 MPa	**32.7 MPa**
	U140 x 75mm	34.6 MPa	31.5 MPa	32.6 MPa	**32.9 MPa**

To test the strength and capacity of the channel sections used in push-out specimens coupon samples were taken from each of the five sections webs'. Results from the coupon tests are summarized in Table.1.8.

Table 1.8 Material Properties of Channel Sections

Channel Size	Yield Strength (MPa)	Tensile Strength (MPa)	Maximum Elongation (%)
UPN 65	422	501	22
UPN 80	364	467	33
UPN 100	332	470	33
UPN 120	344	465	33
UPN 140	318	451	35

1.8.5 Results

In this section results of the ten push-out specimens are presented. As a standard, push-out specimens are compared by load vs. slip information and ultimate load capacity of that shear connector hence results will be displayed as such.

As results showed, there was only one failure mechanism contrary to what other researches shown. All of the specimens were observed to be fail by steel channel web fracture near the fillet (Fig.1.16 and Fig.1.17). Only one specimen showed weld failure (U100 x 75mm).

Figure 1.16 Chanel Fracture – Base Plate

Figure 1.17 Channel Fracture – Concrete Slab

Test results reflected that channel height had significant effect on the ultimate load capacity of the channel shear connector. However higher channel connectors showed close ultimate load capacities. Compressive strength of the concrete starts to dominate the ultimate load capacity thus increasing the channel height becomes futile. Effects of the channel height can be seen from the Fig. 1.18. Figure shows the channel height with respect to the normalized ultimate capacity. Ultimate capacity of the U65 channel is selected as the base criteria.

Additionally, results showed that changing the channel length from 50mm to 75mm increased the ultimate load capacity by a margin of 20 to 35 percent (Fig.1.19). Also when channel length increased visual surface cracking started (Fig.1.20) with higher channels. So this means that at some point channel fracture failure would turn into cracking and splitting failure as previous researchers mentioned.

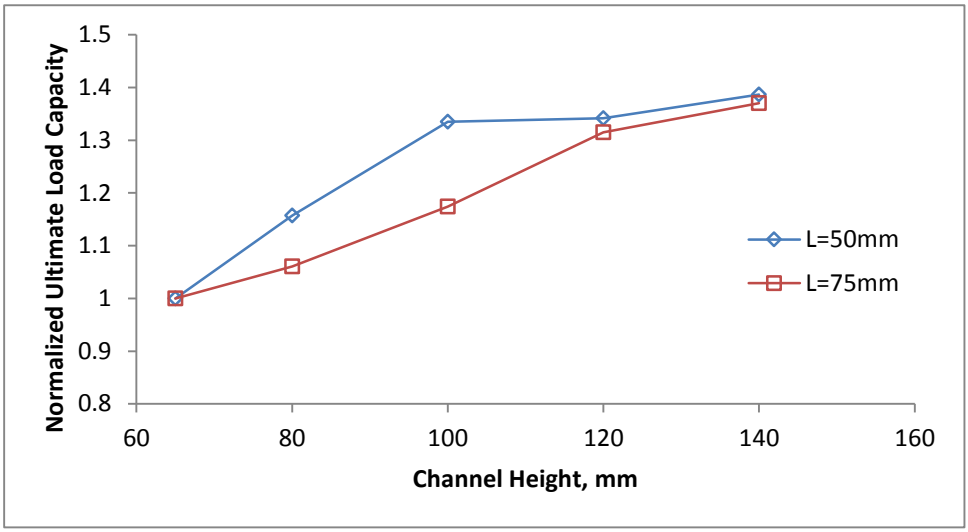

Figure 1.18 Relationship Between Channel Height and Ultimate Load Capacity

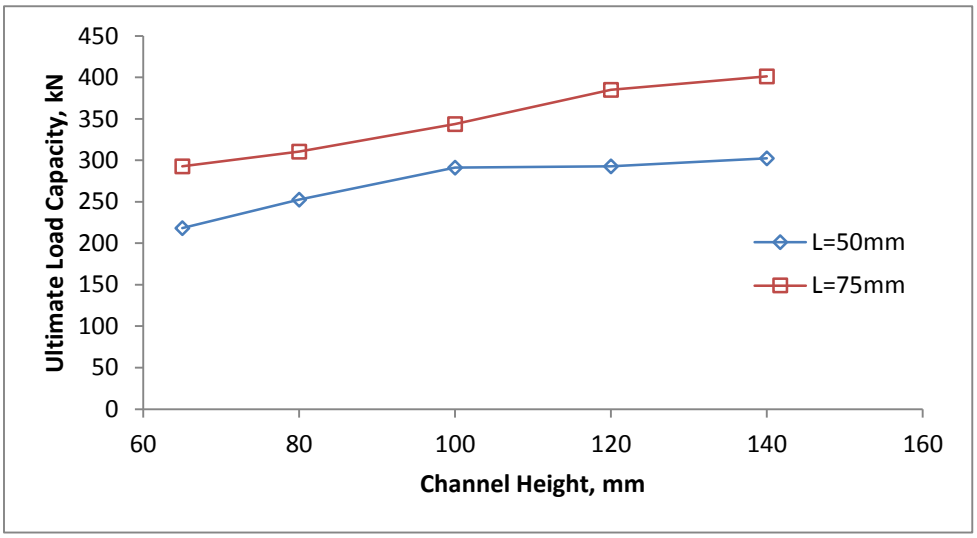

Figure 1.19 Ultimate Load Capacity

Figure 1.20 Surface Cracking – U140 x 75mm

1.9 On Going Research

After the push-out tests, researchers continued with full-scale beam tests. The general aim for that research was to investigate the full and partial composite actions in the composite beams while using channel shear connectors.

Some of the test results were compared with 3D beam models in Chapter 3. However the research was continuing while this thesis was being written thus details could not be given.

1.10 Code Provisions

American (AISC, 2005) and Canadian (CSA, 2001) design codes provide recommendations for composite beam design though most of the provisions include headed studs there are couple of equations that help predicting the ultimate load capacity of channel shear connectors. As it was mentioned before those equations represent only limited range of channel connectors.

The current Canadian design code, CAN/CSA-S16-2001 specifies that, q_{rs} in Eq.1.2 (CSA, 2001), can be used to predict the ultimate load performance of channel shear connectors embedded in solid concrete slab.

$$q_{rs} = 36.5\emptyset_{sc}(t_f + 0.5t_w)L_c\sqrt{f_c'} \qquad \text{(Eq.1.2)}$$

where;
ϕ_{sc} : resistance factor for shear connectors
t_f : flange thickness of channel shear connector (mm)
t_w : web thickness of channel shear connector (mm)
L_c : length of channel shear connector (mm)
$f'c$: compressive cylinder strength of concrete (MPa)

The current American Design code (AISC, 2005) specifies that, Q_n in Eq.1.3, can be used to predict the nominal strength of a channel shear connector embedded in solid concrete slab.

$$Q_n = 0.3(t_f + 0.5t_w)L_c\sqrt{f_c'E_c} \qquad \text{(Eq.1.3)}$$

where;
E_c : modulus of elasticity of concrete (MPa)
Description of other parameters in Eq.1.3 is similar to Eq.1.2.

Additionally there is one other equation provided by Pashan (2006). This equation was generated using 18 push-out specimens with solid concrete slab. This publication specifies that, q_u in Eq.1.4, can be used to predict the ultimate load capacity of channel connectors.

$$q_u = (336w^2 + 5.24LH)\sqrt{f_c'} \qquad \text{(Eq.1.4)}$$

where;
w : web thickness of the channel (mm)

L : length of the channel (mm)
H : height of the channel (mm)
$f'c$: compressive cylinder strength of concrete (MPa)

For comparison these equations were tried and evaluated by the results of the push-out tests done by Baran and Topkaya (2012). As it can clearly be seen from Fig.1.21 provided equations do not represent every channel connector.

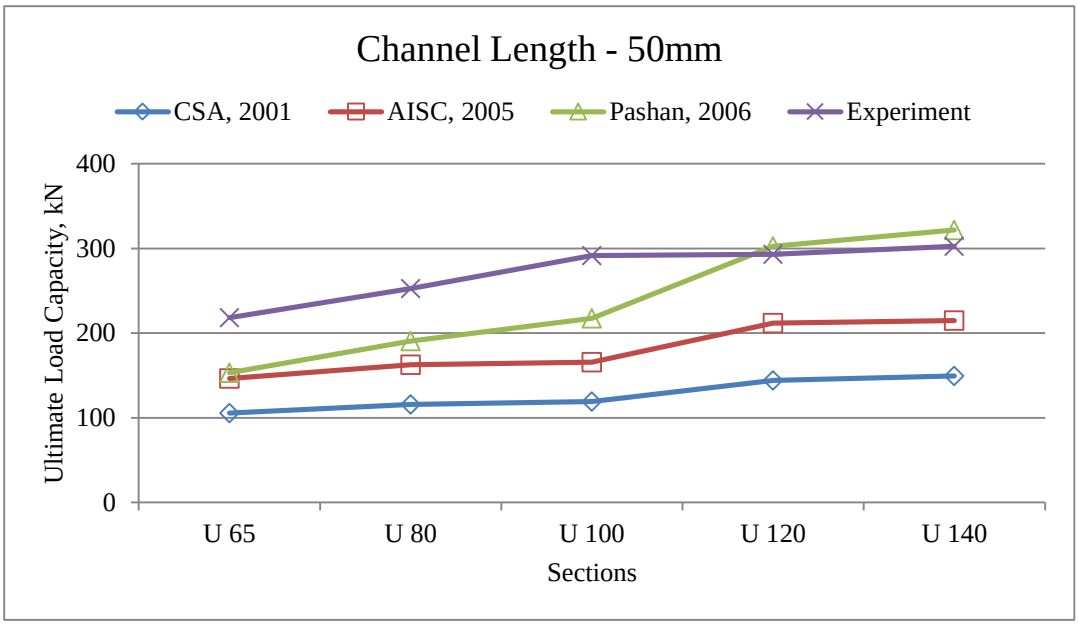

Figure 1.21.a Comparison Between Equations – Channel Length, 50mm

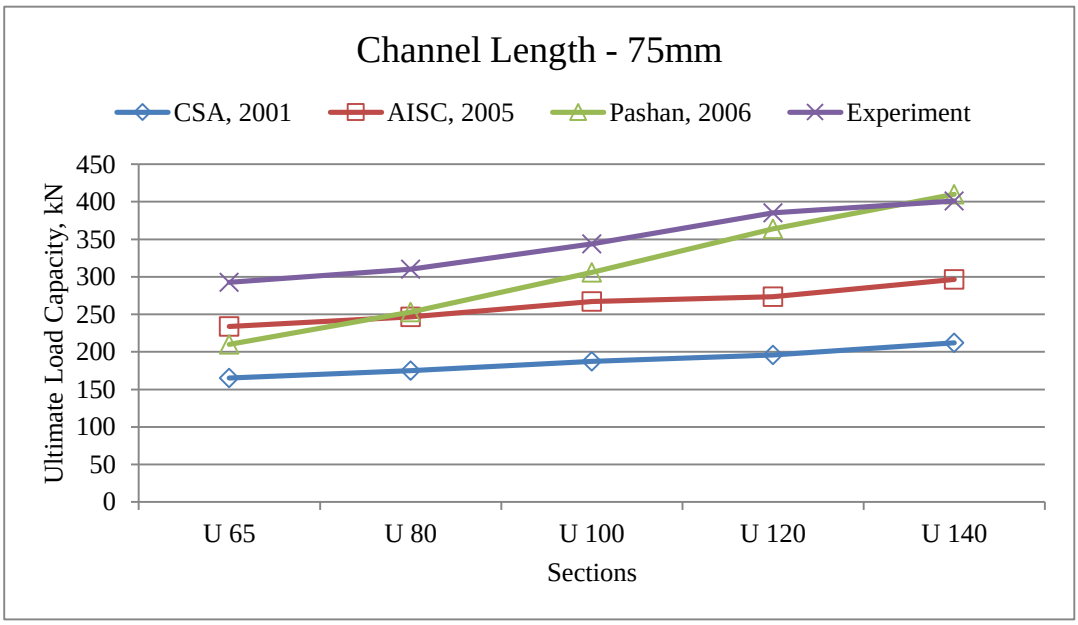

Figure 1.21.b Comparison Between Equations – Channel Length, 75mm

For example channel height range for Pashan (2006) push-out tests were 102 to 127mm and push-out test mentioned in the study by Baran and Topkaya (2012) has a range of 65 to 140mm in channel height. Thus Eq.1.4 predicts the capacity of in range channels with good accuracy, then out of range channels starts to loose accuracy (Fig.1.21).

It can clearly be seen from the Fig.1.21 that all equations that are provided to predict the ultimate load carrying capacity of channel connectors embedded in solid concrete slab presents too conservative results.

However, when it comes to using European channel sections as shear connectors Baran and Topkaya (2012) developed a new inclusive equation with better accuracy. R_n in the Eq.1.5 can be used to predict the ultimate load capacity of channel connectors.

$$R_n = 0.25.F_1.F_2.f_c'.L_c.H + \frac{2+t_w^2.L_c}{H}F_u \qquad \text{(Eq.1.5)}$$

where;
$F_1 : 7.2 - 0.023.L_c$
$F_2 : 1.5 - 0.005.H$
f'_c : compressive cylinder strength of concrete (MPa)
L_c : length of channel shear connector (mm)
H : height of the channel (mm)
t_w : web thickness of channel shear connector (mm)
F_u : tensile strength of steel (MPa)

Accuracy of the Eq.1.5 with the experimental results can be seen from Fig.1.22.

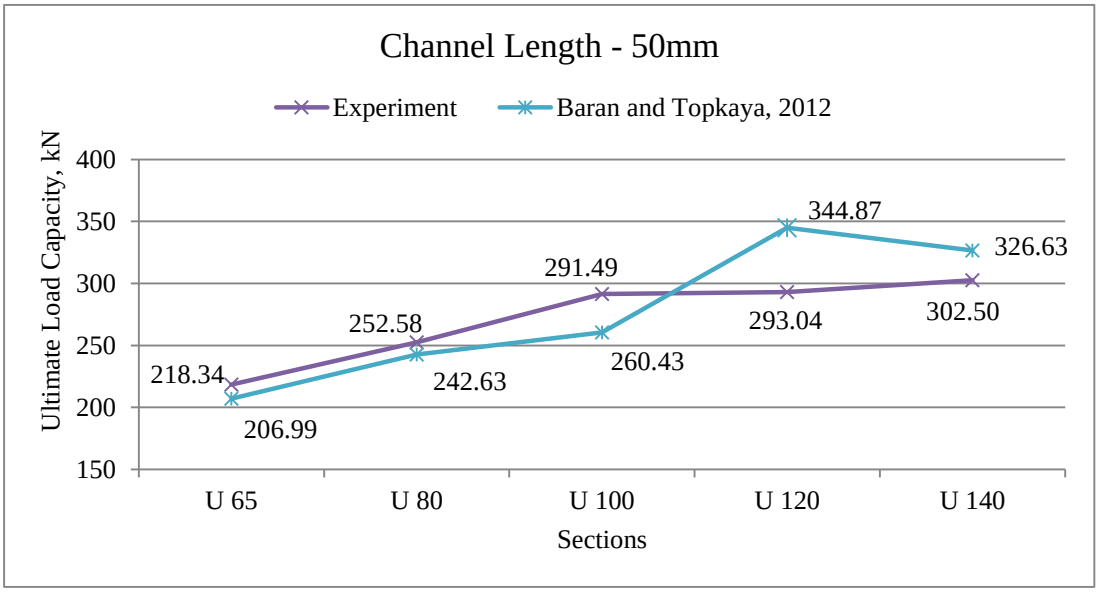

Figure 1.22.a Comparison of Exp. Results and Predicted Load Capacities Using Eq.1.5

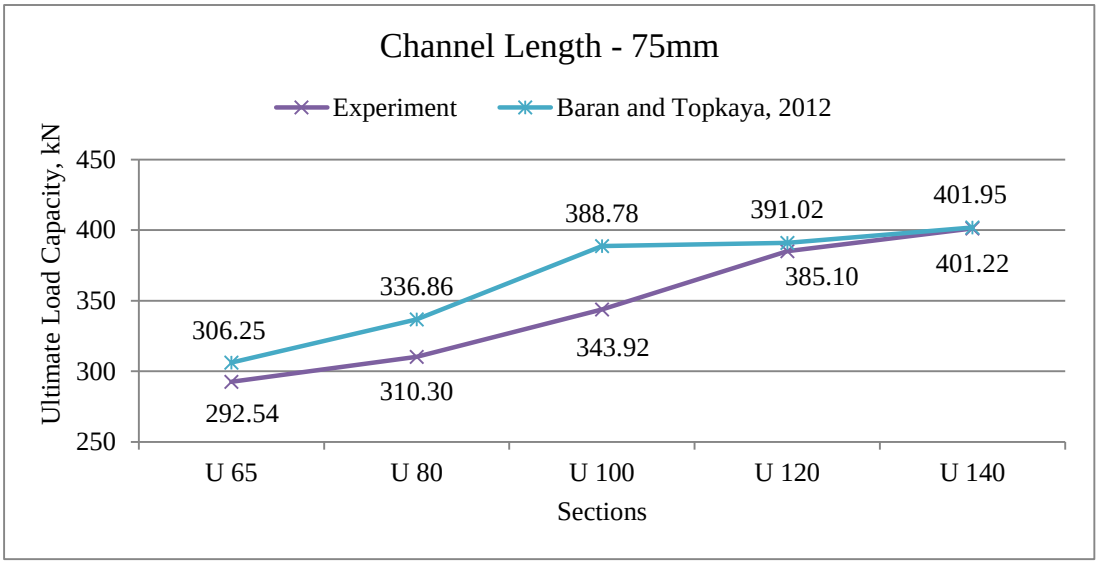

Figure 1.22.b Comparison of Exp. Results and Predicted Load Capacities Using Eq.1.5

1.11 Problem Statement and Organization of the Thesis

The only knowledge about the behavior and ultimate load capacity of the channel shear connectors are limited to the experimental data from previous researches. However experimental programs are costly and time consuming. These are the main disadvantages of alternative shear connector researches.

With the improvements toward mathematical modeling it is becoming more and more possible to use finite elements models to simulate the experimental programs. On the other hand, there are still challenges with modeling concrete as a nonlinear material.

This thesis focuses on simulating the push-out (Baran and Topkaya, 2012) and full-scale beam tests using commercially available finite element modeling program called ANSYS V13.0. Using ANSYS Mechanical APDL language 2D and 3D models were created. 2D models were used to simulate the previously mentioned push-out tests while full-scale beam tests were simulated using 3D models. Several nonlinear concrete modeling approaches have been tried in these models. Some concrete modeling approaches were successful for mimicking the concrete behavior and their results were in acceptable limits. However, other concrete modeling approaches which are being used more commonly did not give results as expected.

Chapter 2 of this thesis presents details through making the 2D model and evaluates the accuracy of the model by comparing the push-out test results to FEA results.

Chapter 3 presents several concrete modeling methods used in the 3D model, compares the results of different methods and comments on their behavior, then assesses the difference between FEA results that uses more successful modeling approach and full-scale beam test results. Full-scale beam tests are continuing while this thesis is being written.

Chapter 4 presents conclusions and future research aspects.

CHAPTER 2

PUSH-OUT TEST SIMULATION USING 2D FE MODELS

2.1 Preamble

There are limited amounts of work on simulating push-out test specimens including channel sections as shear connectors. One of the research papers was mentioned in Chapter 1; (Maleki and Bagheri, 2008) a 3D model to examine some parameters and their effects on the ultimate capacity. As the previous studies resulted that the relationship between channel length and the ultimate capacity had shown a fairly linear correlation. Is it possible for a 2D analysis to give satisfactory results on push-out test specimen's behavior?

This chapter of the thesis presents 2D models created by ANSYS v13.0 using plane elements and simplistic material models. The dimensions used in these models were same as the push-out specimens mentioned in Chapter 1; the specimens with European channel sections as shear connectors. Using plane elements and simplifying the model gives advantage over 3D modeling on time consumption during modeling and analysis stages. At the end, results from the FEM's and push-out tests were compared and reviewed by their performances.

2.2 Element Types

Both of the mediums, concrete slab and channel connector, had been modeled with PLANE42 elements. This element has four nodes with two degree of freedoms on each node and is used for 2D modeling of the solid structures. Also the element is capable of plasticity and large deflections. Plane element was used in plain strain by setting the KEYOPT(3) option to 2. A schematic for this element is given in Fig.2.1.

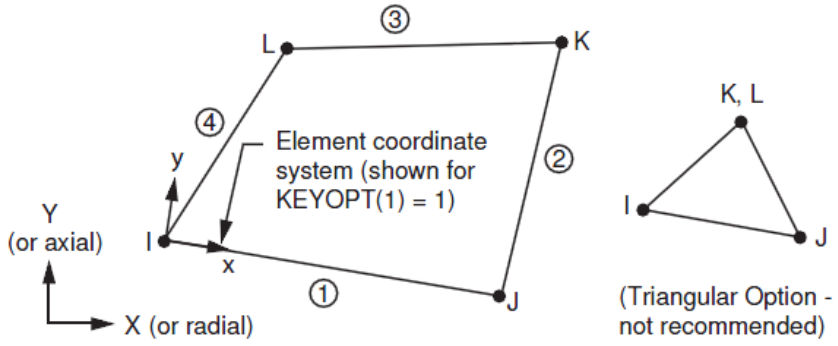

Figure 2.1 PLANE42 Geometry (Ref: ANSYS, 2010)

To represent the interaction and physical contact between concrete slab and channel connector target and contact elements should be used. TARGE169 and CONTA171 elements

are employed for this purpose. TARGE169 is a 2D target segment and used to represent 2D target surfaces for associated contact elements. Any transitional or rotational displacements also forces and moments can be imposed on target segments. On the other hand, CONTA171 is a 2D two node surface to surface contact element and used to represent contact and displacement between 2D target surfaces. Schematics for both elements are shown in Fig.2.2.

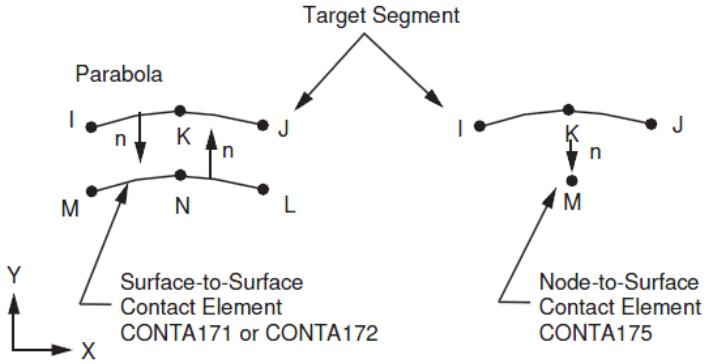

Figure 2.2.a TARGE169 Geometry (Ref: ANSYS, 2010)

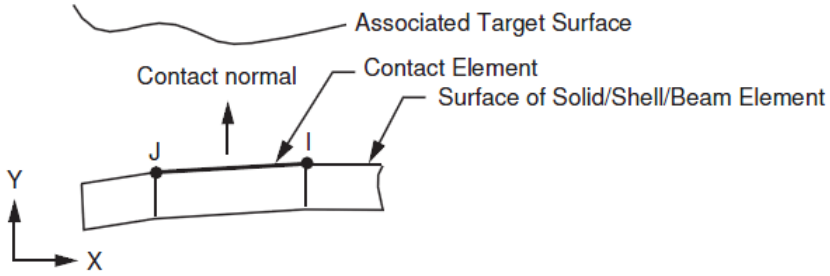

Figure 2.2.b CONTA171 Geometry (Ref: ANSYS, 2010)

More detailed information about the elements can be found in ANSYS User's Guides (ANSYS, 2010).

2.3 Material Properties

Needed parameters for defining the material models can be found in Table 2.1. As it can be seen from the table both material models consist of two parts. Both steel channel connector and concrete slab was modeled as bilinear.

Material Model 1 was used to model steel channel connector. PLANE42 requires linear isotropic and bilinear kinematic properties to properly model the steel material. Bilinear material model is based on von Mises failure criteria. EX is the elasticity modulus of the channel connectors (E_s *: 200GPa*) and PRXY is the Poisson's ratio (ν *: 0.3*). Bilinear model also requires the yield strength (f_y) and the hardening modulus of the steel. The yield stress for all channel connectors was taken as 320MPa, and the hardening modulus was 2GPa as 1% of the elasticity modulus (Table 2.1).

Material Model 2 was used to model the concrete slab. To model concrete as simple as possible bilinear material model was chosen. Elasticity modulus of the concrete slab (E_c) was calculated separately for every specimen of the push-out test. The modulus of elasticity was based on the Eq.2.1.

$$E_c = 0.04272.w_c^{1.5}\sqrt{f_c'} \quad (2.1)$$

where;
w_c : unit weight of the concrete (taken as 2400 kg/m^3)

As before bilinear model requires the ultimate strength of the concrete (*f'c*) also the hardening modulus. Ultimate strengths were taken from the push-out test (Table1.7) and hardening modulus was calculated as 1.5% of the elasticity modulus for every specimen (Table 2.2).

Table 2.1 Material Properties for U65 - 50mm Model

Material Model	Element Type	Material Properties	
1	PLANE42	Linear Isotropic	
		EX :	200 GPa
		PRXY :	0.3
		Bilinear Kinematic	
		Yield Stress :	0.32 GPa
		Tang. Mod. :	2 GPa
2	PLANE42	Linear Isotropic	
		EX :	28.53 GPa
		PRXY :	0.25
		Bilinear Kinematic	
		Ultimate Stress :	0.0318 GPa
		Tang. Mod. :	0.4279 GPa

Density is not required for modeling, hence was not added to the material model.

2.4 Modeling

Push-out tests included ten specimens divided into two cases, as it was mentioned in Chapter 1 before. The test specimens were simplified to a 2D geometry and modeled as areas. Model dimensions were same as the push-out test and simplified geometry resembles Section A-A in the Fig.1.11. Concrete slab was 70cm long and 18cm thick and channel connectors were embedded in the concrete slab. However, FE analysis for every specimen was done in two separate models. One of the models was called Untapered Model (UM) and the other one called Tapered Model (TM). The only difference between models was the channel dimensions.

Table 2.2 Necessary Concrete Properties For Modeling

	Properties of Concrete		
Specimen	Ec (Gpa)	fc' (MPa)	Hardening Modulus (GPa)
U65 - 50mm	28.53	31.83	0.4279
U80 - 50mm	29.16	33.27	0.4374
U100 - 50mm	28.69	32.20	0.4303
U120 - 50mm	31.92	39.85	0.4787
U140 - 50mm	30.64	36.73	0.4596
U65 - 75mm	29.75	34.63	0.4463
U80 - 75mm	29.39	33.80	0.4409
U100 - 75mm	30.07	35.37	0.4510
U120 - 75mm	28.91	32.70	0.4337
U140 - 75mm	29.00	32.90	0.4350

Table 2.3 Modeling Summary

	Specimens	Models		
Case 1	U65-50mm U80-50mm U100-50mm U120-50mm U140-50mm	*Untapered Model, (UM)	*Tapered Model, (TM)	*Same Boundary Conditions *Same Loads *Same Mesh Density *Same Material Properties
Case 2	U65-75mm U80-75mm U100-75mm U120-75mm U140-75mm	*Untapered Model, (UM)	*Tapered Model, (TM)	

UM uses the same dimensions given in Chapter 1 which are from European section catalogs and modeled as simple rectangular areas. On the other hand, real channel section dimensions slightly differ from those tabulated values. Additionally, flange thickness is not constant all the way through. It decreases from web side to the tip. Both of the channel geometries are shown in Fig.2.3.

Dimensions of channel sections used in push-out tests (Baran and Topkaya, 2012) are measured and TM was created according to those measurements. TM dimensions of Baran and Topkaya (2012) are given in Table 2.4.

Table 2.4 TM Dimensions

Section	Channel Section Properties				
	Height, H (mm)	Flange Width, W (mm)	Web Thickness, s (mm)	Flange Thickness, (mm)	
				a	b
UPN 65	65	42	5.5	6.7	8.6
UPN 80	80	45	6	7	9.1
UPN 100	100	50	6.5	7.2	9.6
UPN 120	120	55	7.5	7.21	10.5
UPN 140	140	60	7.5	8.1	11.8

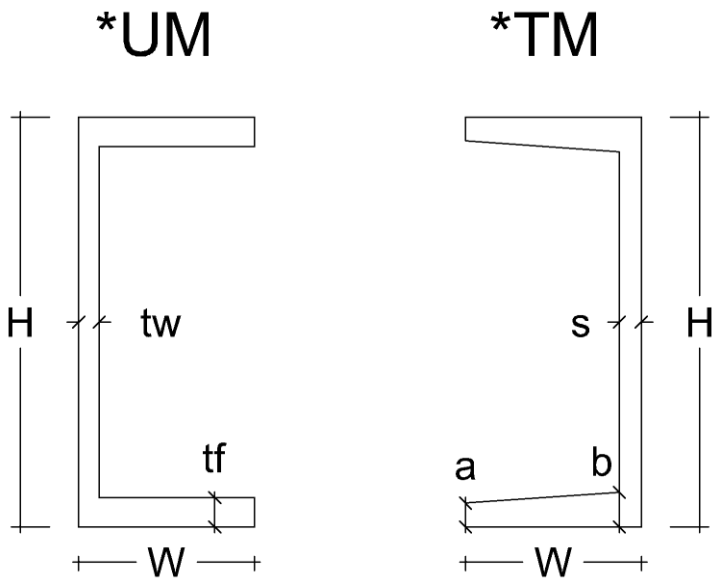

Figure 2.3 Two Different Channel Models
Untapered Model, UM (left hand side)
Tapered Model, TM (right hand side)

Other than channel geometry there were no differences between models; same mesh densities, material properties, load and boundary conditions.

First channel connector was modeled as areas, and then concrete slab was modeled around the channel connector. However instead of modeling a base plate forces acting on steel connector were applied directly to the bottom flange of the channel. Combined areas can be seen in Fig.2.4. FE meshed geometry is shown in Fig.2.5.

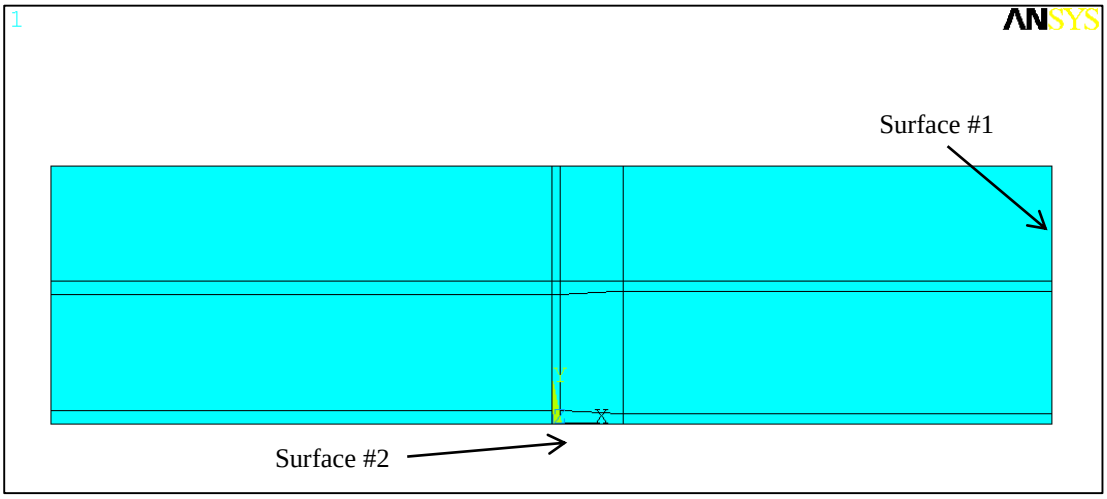

Figure 2.4 Combined Areas in ANSYS (*TM)

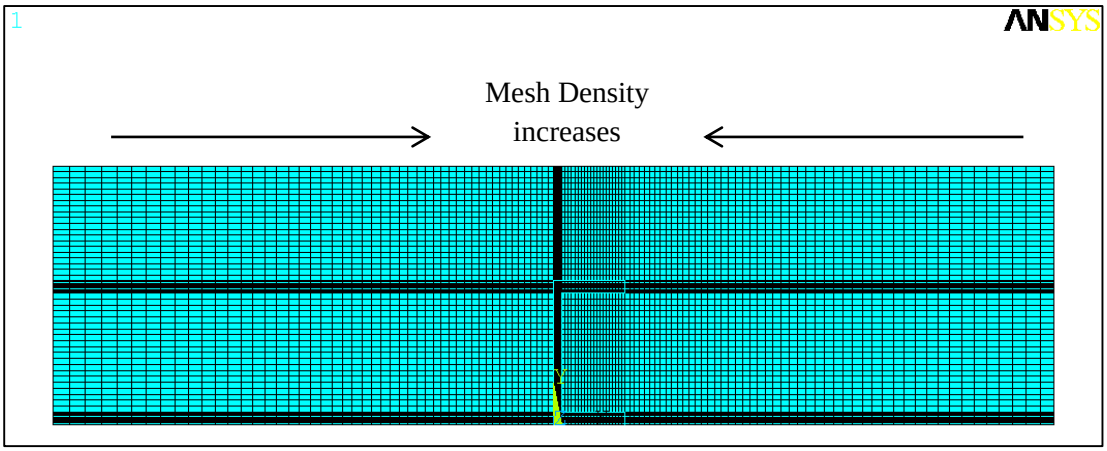

Figure 2.5 Meshed Geometry in ANSYS (*UM)

2.5 Meshing

To generate good results ANSYS recommends using rectangular meshes for PLANE42 element. Thus, area mesh was set up in a way to create rectangular areas. After creating the areas, lines were divided using LESIZE command so when free meshing was employed these divided lines would be the base for meshing. Using this command channel flange and web thicknesses were divided into 10, channel height and flange width were divided into 20 pieces.

Previous attempts showed that couple of areas should be densely meshed to get more satisfying results. According to that mesh density was increased near the interaction surfaces; near the contact surfaces (Fig.2.6). From outside of the model to inside mesh density increases by three times.

2.6 Target and Contact Surfaces

As it was mentioned before main interaction happens between concrete slab and the channel connector, thus employing TARGE169 and CONTA171 elements help simulating the physical contact between two mediums. These elements interact and transfer loads to each other as long as there is a physical contact or predefined condition. After steel connector yields the space between concrete and channel increases and load transfer is only possible for contact surfaces.

In these models channel connector surface was set as target surface that resists the forces transferred by contact elements, and so concrete slab surface touching the channel surface was set to be the contact surface that pushes against the channel faces and flanges (Fig.2.6). Target and contact surfaces coincide yet defined as separate surfaces.

2.7 Loads and Boundary Conditions

Base plate was not modeled thus using displacement boundary conditions model was needed to be constrained to mimic the function of the base plate. Base plate prevented the specimen from moving up and displacing in the test setup. By this logic surface number one (Fig.2.4), the right hand side of the model, was constrained towards moving in both X and Y directions (Fig.2.7).

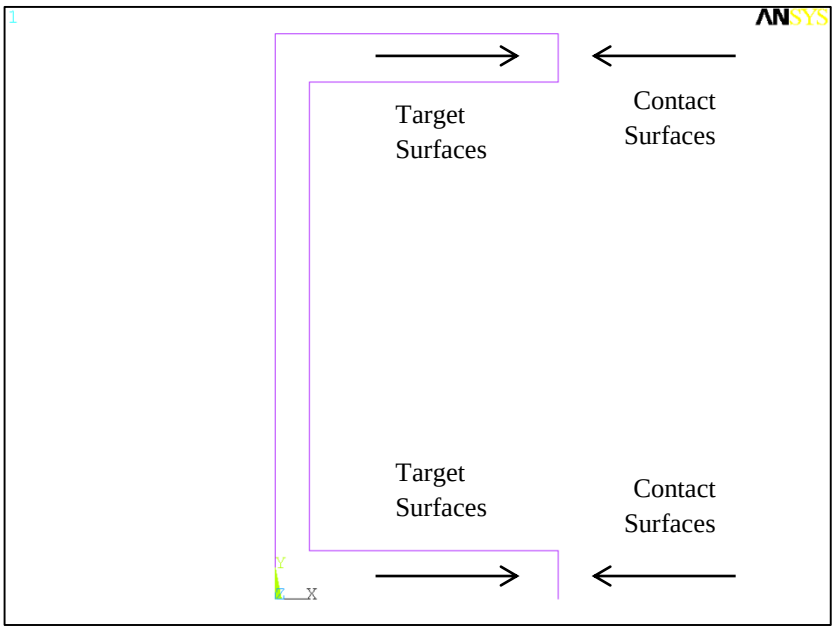

Figure 2.6 Target & Contact Surfaces

Additionally surface number two, bottom of the model, was constrained in Y direction so that the concrete and channel connector would resist the up lift forces generated after steel member yields (Fig.2.7).

Finally load from the machine was applied directly to the bottom of the channel connector as displacement to consider the nonlinear effects and against convergence problems.

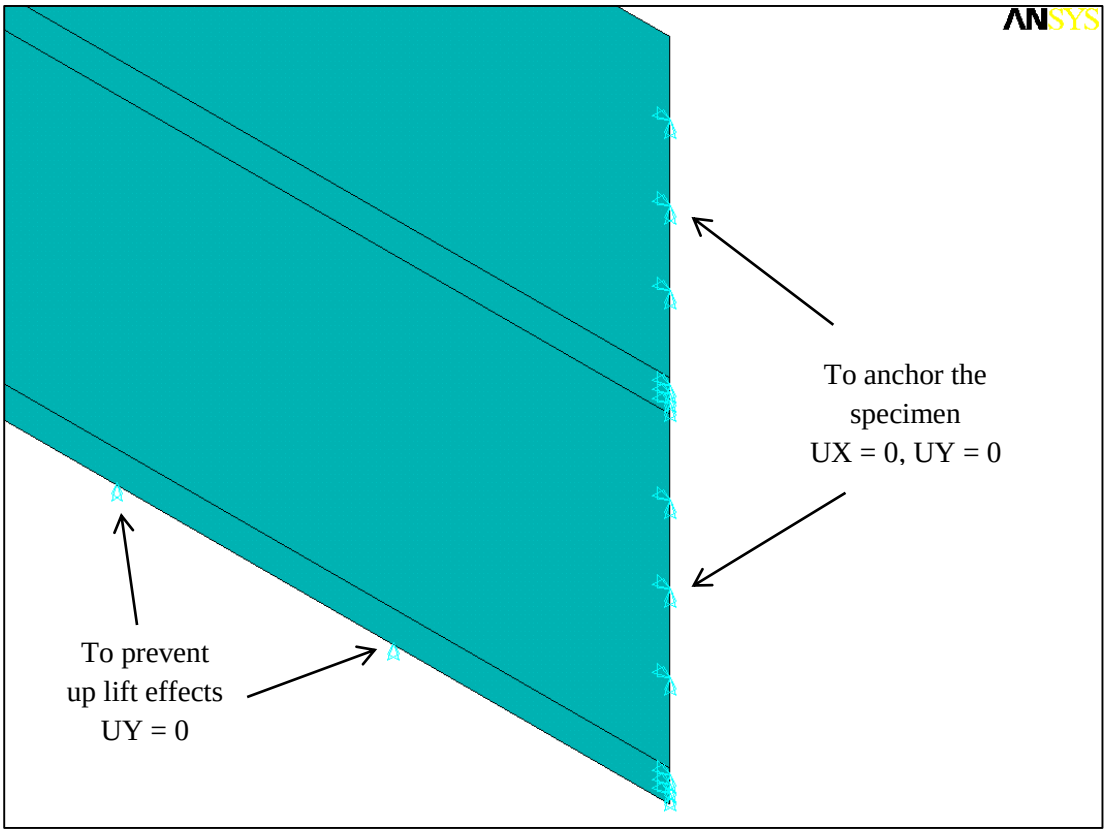

Figure 2.7 Boundary Conditions

2.8 Analysis and Solution Control

For every analysis in ANSYS solution control commands control the linear and nonlinear solution options. In all models, the typical commands used for nonlinear static analysis were listed in Table 2.5.

Nonlinear geometry was considered for the push-out specimens thus analysis was set as large displacement and static. With activating line search method solution method was set as Newton-Raphson Method. This method uses several substeps to apply the load (displacement) gradually. Further technical details about this method and solution process can be found in ANSYS User's Guides (ANSYS, 2010).

Other solution control commands that were not mentioned in here were set as program defaults. After the analysis program was set to terminate and exit the solution.

Table 2.5 Basic Sol'n Control Commands

Analysis Options	
Large Displacement Static	Yes
Calculate Prestress effects	No
Time Control	
Automatic Time Stepping	Program Chosen
Number of Substeps	5000
Max Num. of Substeps	100000
Min Num. of Substeps	10
Write Items to Results File	
All Solution Items	Yes
Frequency	Write Every Substep

2.9 Results

The goal of these analyses was to evaluate the 2D modeling capabilities in ANSYS v13.0 and assess the results whether they are in reasonable margins or not. Therefore a fractured channel section used in push-out tests (Baran and Topkaya, 2012), U100-75mm, was compared with its associated FE model. Deformed shape of the model resembles the fractured channel and it can be seen in Fig.2.8.

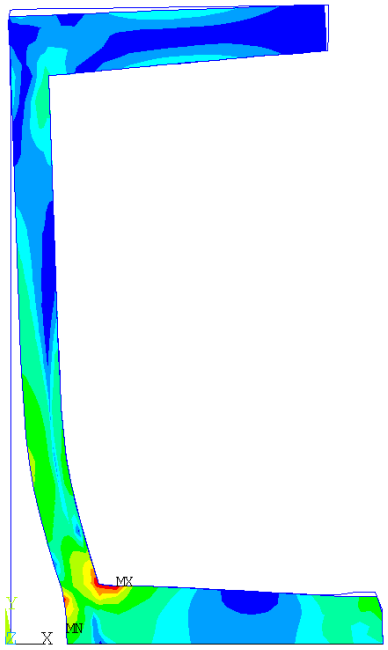

Figure 2.8 U100-75mm Deformed Shape

Results of the analyses were compared with the load vs. slip data collected from the experiments. Even though models are in 2D, results give a good correlation with push-out test data. The next section includes comparisons and comments. Results from the models and the experiments are plotted in graphs to show the comparison.

2.10 Comparisons

This section compares and comments on the results of the FE analyses. Results are given in the form of a graph and every one of them includes the same aspects. Every graph contains the results from experimental study and FE analysis yet one channel with a specific length (50mm or 75mm) at a time. Additionally, each channel was represented with two FE models; UM and TM. Consequently, each graph constitutes as a summary.

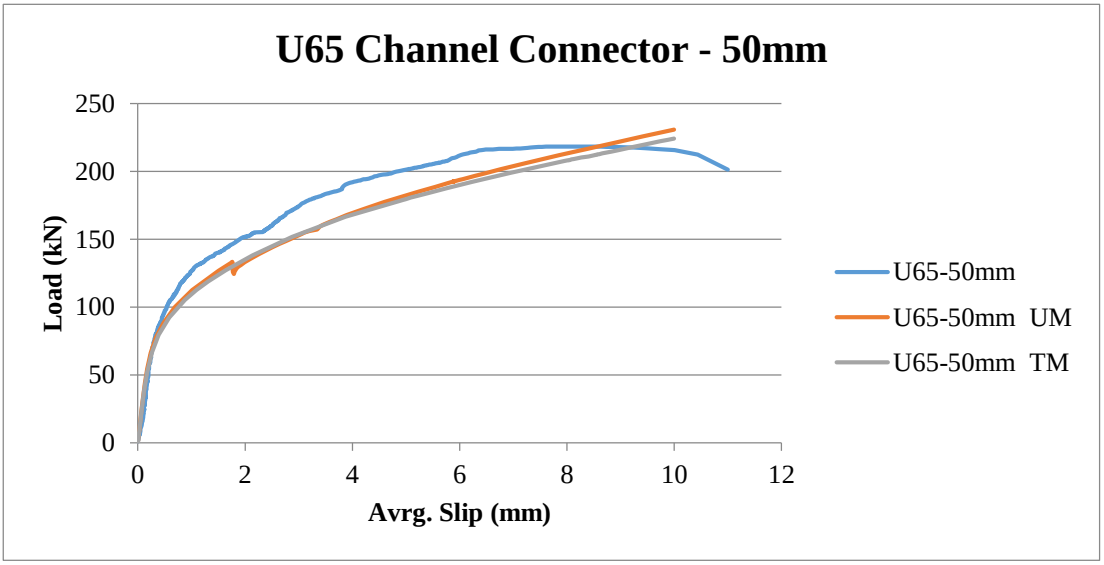

Figure 2.9.a U65 Channel Connector Results for 50mm Length

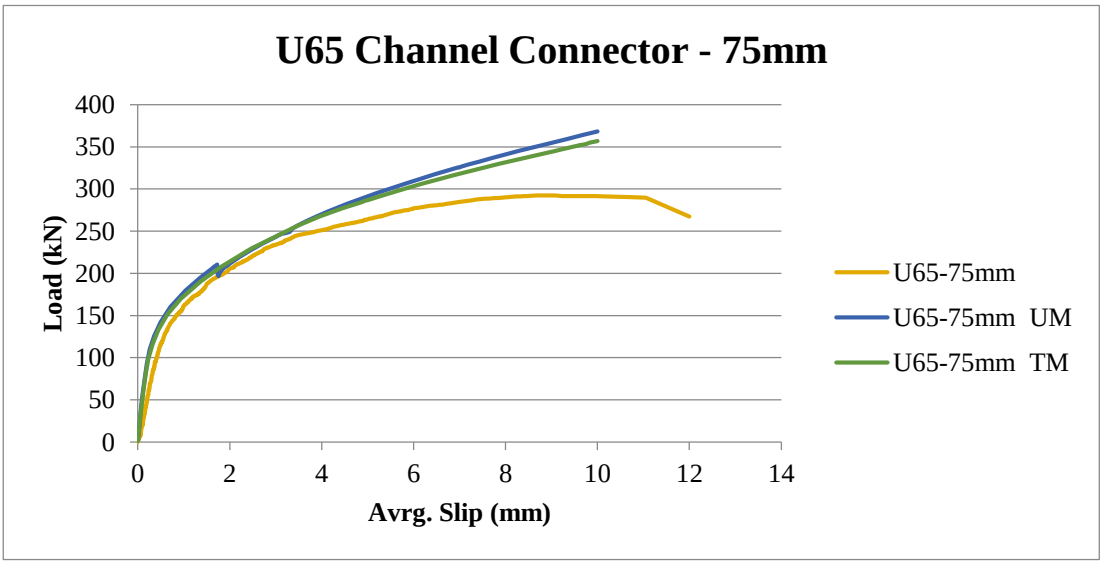

Figure 2.9.b U65 Channel Connector Results for 75mm Length

As a start U65 channel connector results were given in Fig.2.9. It is clear from the figure that 2D models for U65 given satisfactory results. Results from the two models, UM and TM, were nearly the same. Initial slope of the graphs showed that linear representation of the models match the experimental behavior. Models of 50mm channel length started yielding a bit early from the test. However, 75mm models showed the same yielding behavior as the push-out test. Yet, material models for concrete did not include the cracking and crushing failure effects so it was expected for analysis results to increase even after concrete starts to crack. Nevertheless, within limits results showed a good correlation for both 50 and 75mm channel lengths.

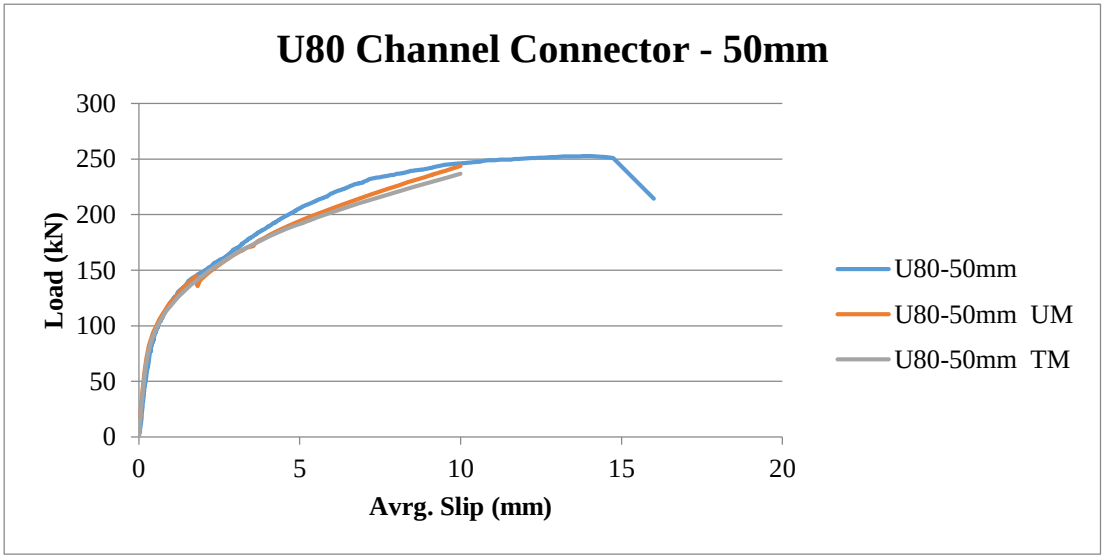

Figure 2.10.a U80 Channel Connector Results for 50mm Length

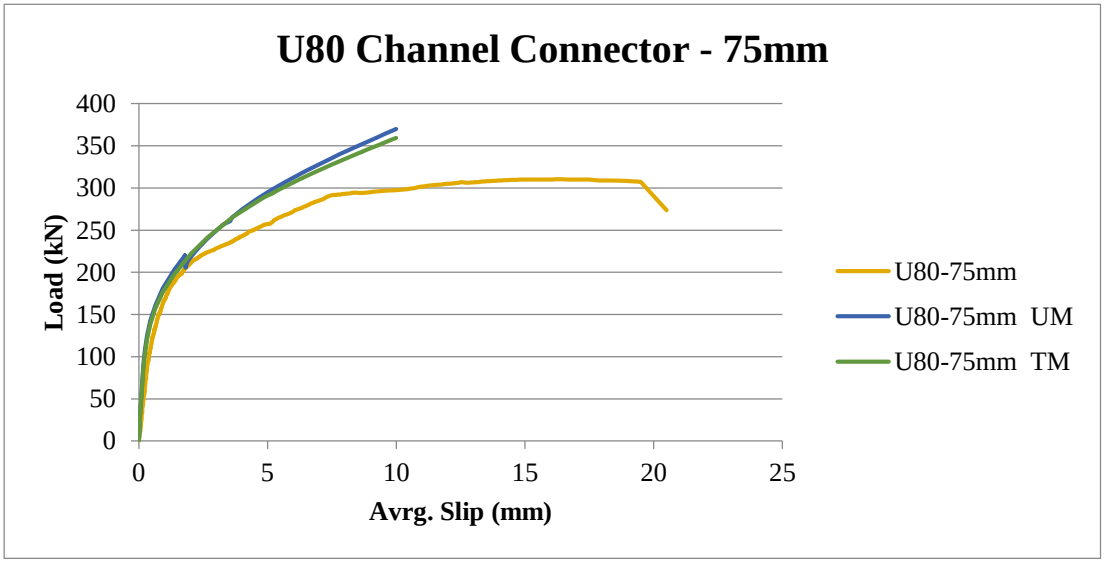

Figure 2.10.b U80 Channel Connector Results for 75mm Length

The second specimen was U80 channel connector and results from the associated models were plotted on Fig.2.10. As before, results of the UM and TM models showed no noticeable difference. This time at initial slope and after yielding, both 50 and 75mm models matched the push-out test results. Though, when concrete cracking started models for 75mm channel connector showed continuing increase. Despite the last part, FE models were good representatives for the push-out tests. Cracking and crushing was not included in the models and some difference was expected yet so far models were in good correlations with their experimental counter parts.

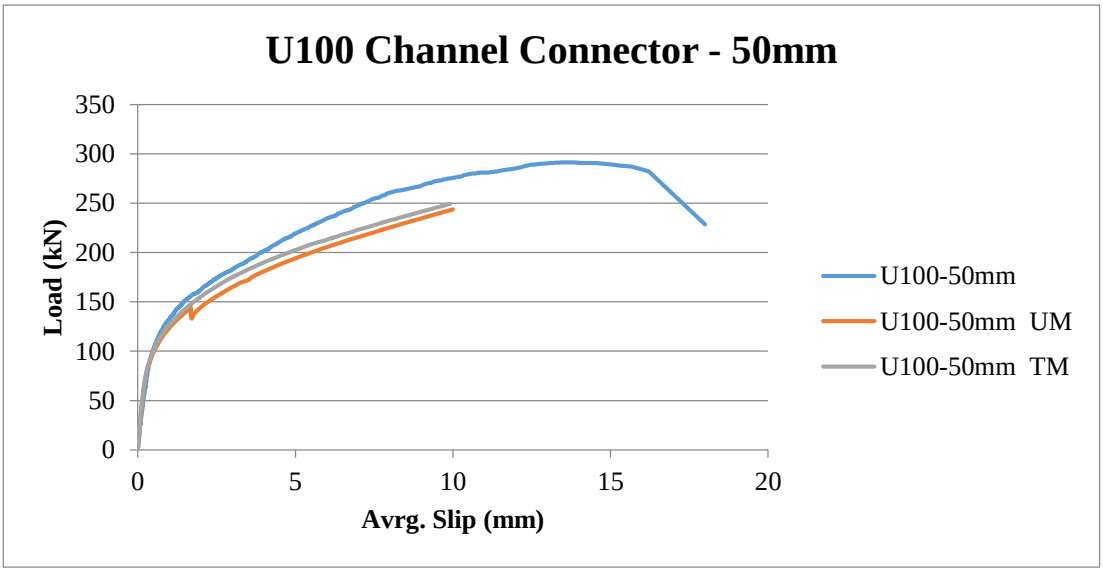

Figure 2.11.a U100 Channel Connector Results for 50mm Length

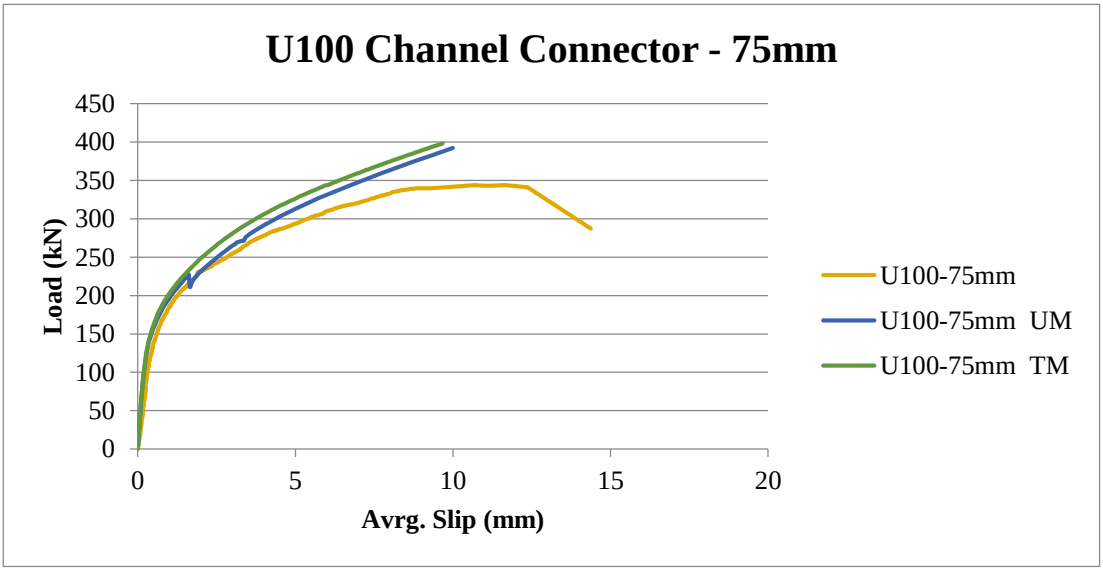

Figure 2.11.b U100 Channel Connector Results for 75mm Length

The third test specimen was U100 channel connector and experimental data with FE model results were plotted on Fig.2.11. With U100 channel connector TM's started to give slightly higher results than UM's. As mentioned before initial slope and after yielding behaviors were acceptable matches for both 50 and 75mm push-out test results despite the concrete cracking failures. Chapter 1 mentioned a weld failure with 75mm channel connector which resulted in early failure. However both models were still in good correlation with the experimental data.

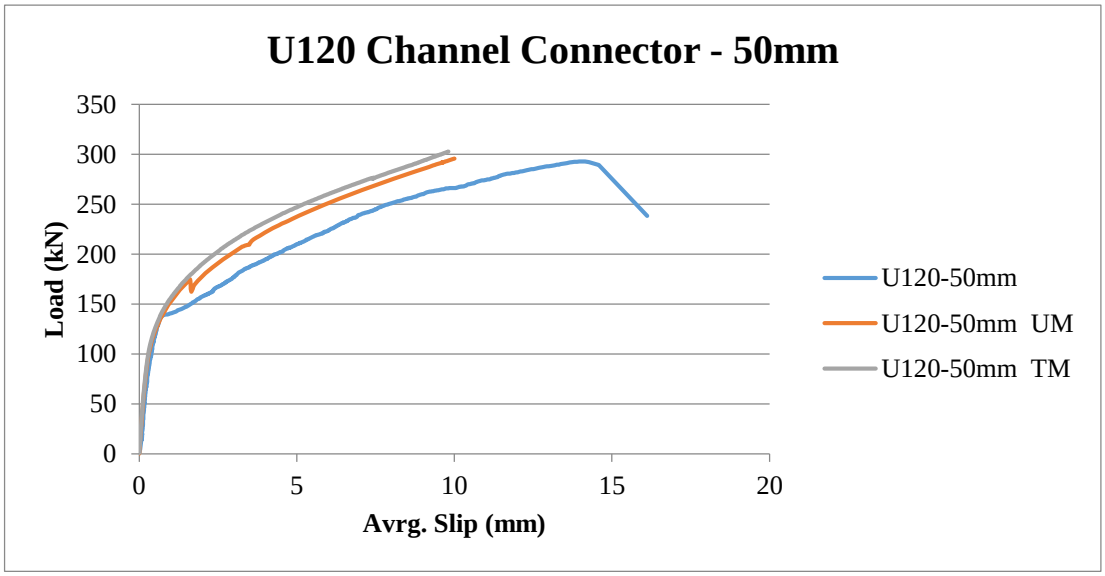

Figure 2.12.a U120 Channel Connector Results for 50mm Length

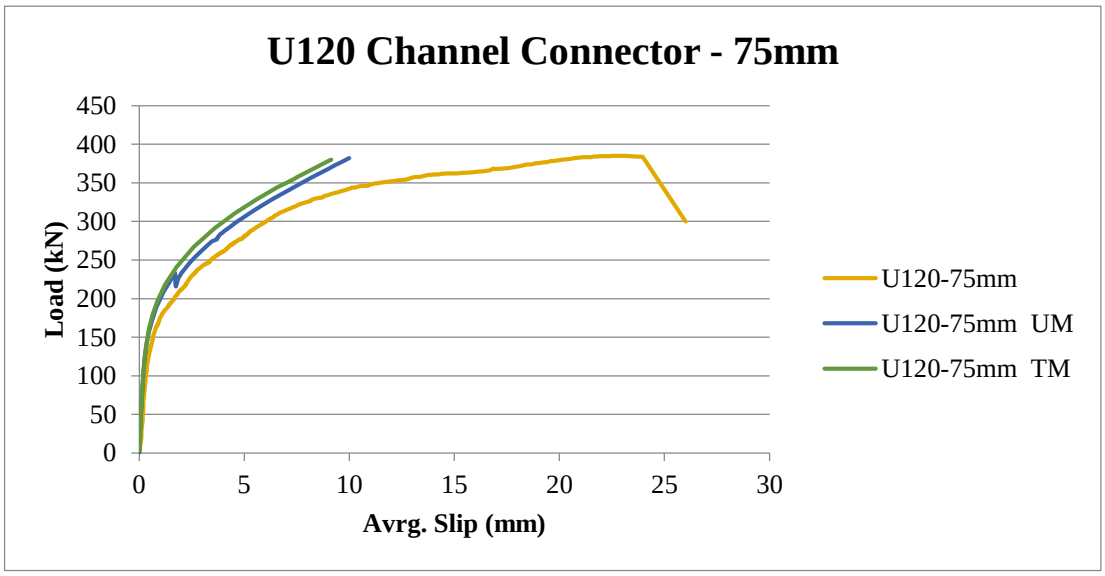

Figure 2.12.b U120 Channel Connector Results for 75mm Length

The next channel connector was U120 and push-out test results with associated FE models results were plotted on Fig.2.12. There was a noticeable difference in experimental results for 50mm channel length. After a linear behavior there is a sudden slip and this was not the case for previous channel connectors. As before models matched the initial slope but after yielding results started separating. Differences between models and the test were higher for 50mm channel length.

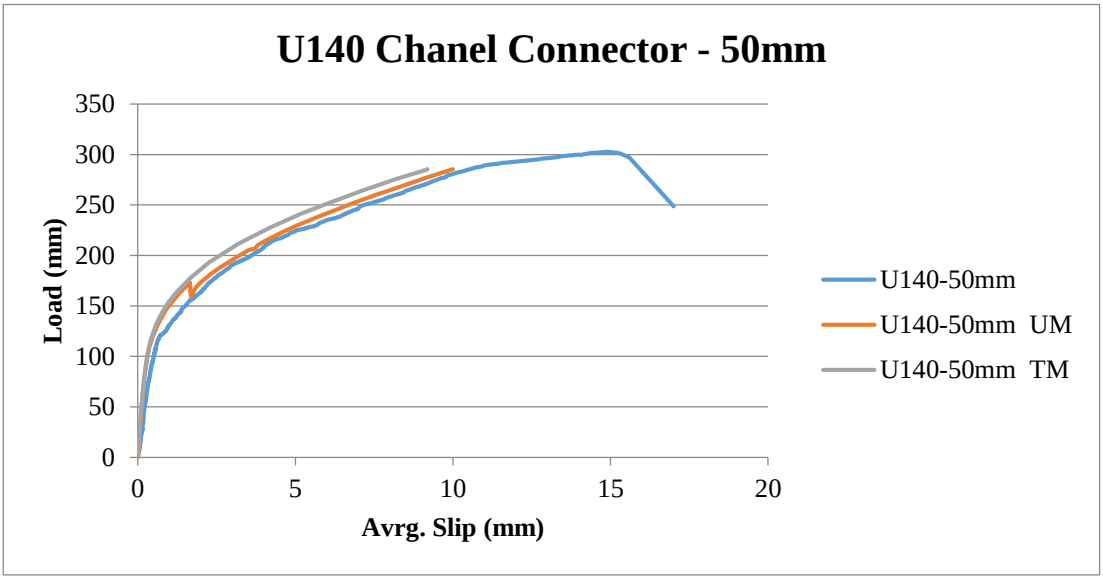

Figure 2.13.a U140 Channel Connector Results for 50mm Length

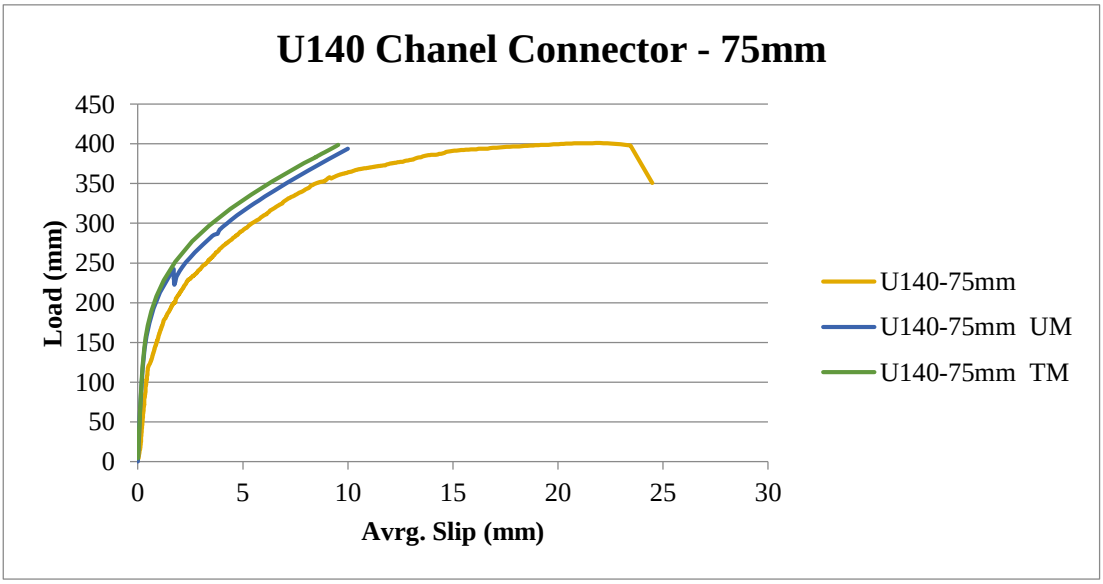

Figure 2.13.b U140 Channel Connector Results for 75mm Length

The final channel connector was U140 and experimental results with necessary FE model results were plotted on Fig.2.13. Just like U120 and U100, TM results were slightly higher than UM results. During the initial slope and after the yielding 50mm channel length results were very satisfactory even after concrete cracking. However, 75mm channel length models started with a little difference in initial slope. Also, after the yielding that difference remained. Despite the good correlation of 50mm channel length test results with its associated FE models, models of 75mm channel length showed noticeable difference.

Comparing the FE models and experimental results showed that 2D modeling has its advantages. Also results were in good correlation at initial slope and yielding stages. However, when concrete slab started cracking some of the models showed continuing increase, instead of limiting to the ultimate load. This showed that modeling concrete using bilinear material models has limitations.

In Chapter 3, several other concrete material modeling approaches were tried in full-scale beam models.

CHAPTER 3

MODELING OF FULL AND PARTIALLY COMPOSITE BEAMS USING 3D FE MODELS

3.1 Introduction

The mechanics of composite actions which are complete interaction (Fig.1.3) and no interaction (Fig.1.2) were mentioned in Chapter 1. For a long time, shear connector calculations were made for full composite action which requires many connectors and allows almost no slip. However, after a while researchers figured out that there was another way to get accurate and economical composite response which is called partial composite action. Using fewer amounts of shear connectors, it was still possible to maintain a serviceable composite action without losing more than 10 to 15% ultimate load capacity.

This chapter of the thesis presents 3D models of the full-scale beam tests done by Baran and Topkaya. The main purpose for these tests was to investigate the full and partial composite actions in the composite beams while using channel shear connectors. Four full-scale beam combinations were generated using various numbers of shear connectors. To simulate their behavior 4 FE models were created using ANSYS v13.0 with a couple of concrete modeling approaches.

At the end, results from the FE models and tests were compared and commented on. Additionally, in the processes many concrete models were tried and most of them failed, some of them are mentioned in this chapter.

3.2 Full-Scale Beam Tests

For full-scale beam tests four specimens were prepared. Specimens consisted of U65x50mm channel connectors that welded on top flange of a steel girder and embedded in concrete slab. Each beam was 3.6m long. The concrete slab was 10cm thick and 80cm wide and also the steel girder was IPE240. Dimensions of the specimen are shown in the Fig.3.1.

Four specimens were prepared with various numbers of channel connectors (Fig.3.2). From specimen number one to number four channel connector density increases. So, number one being the least dense and number four being the most, specimens become fully composite with the increasing specimen number.

A concentrated load was applied to the middle of the simply supported beams and deflection due to this force was recorded during the tests. In addition, end slip values versus the applied load were recorded, too.

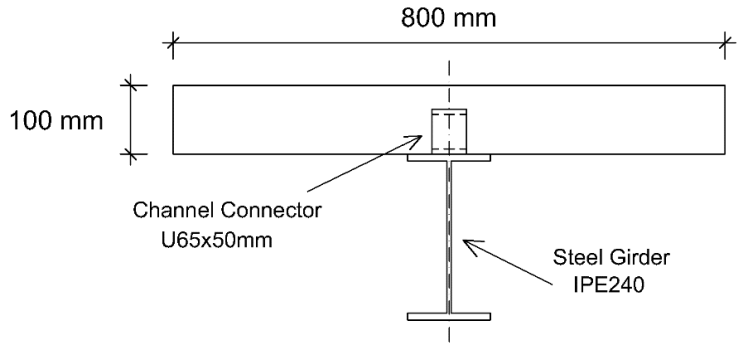

Figure 3.1.a Cross-Section of the Beam Specimen

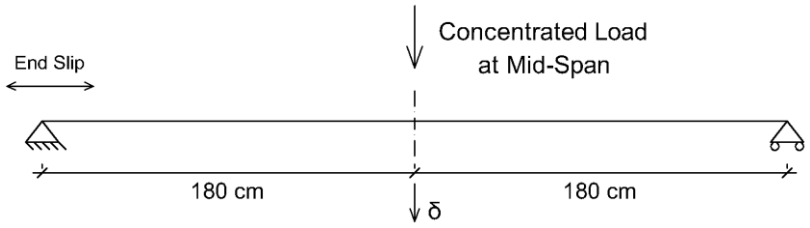

Figure 3.1.b Beam Dimensions

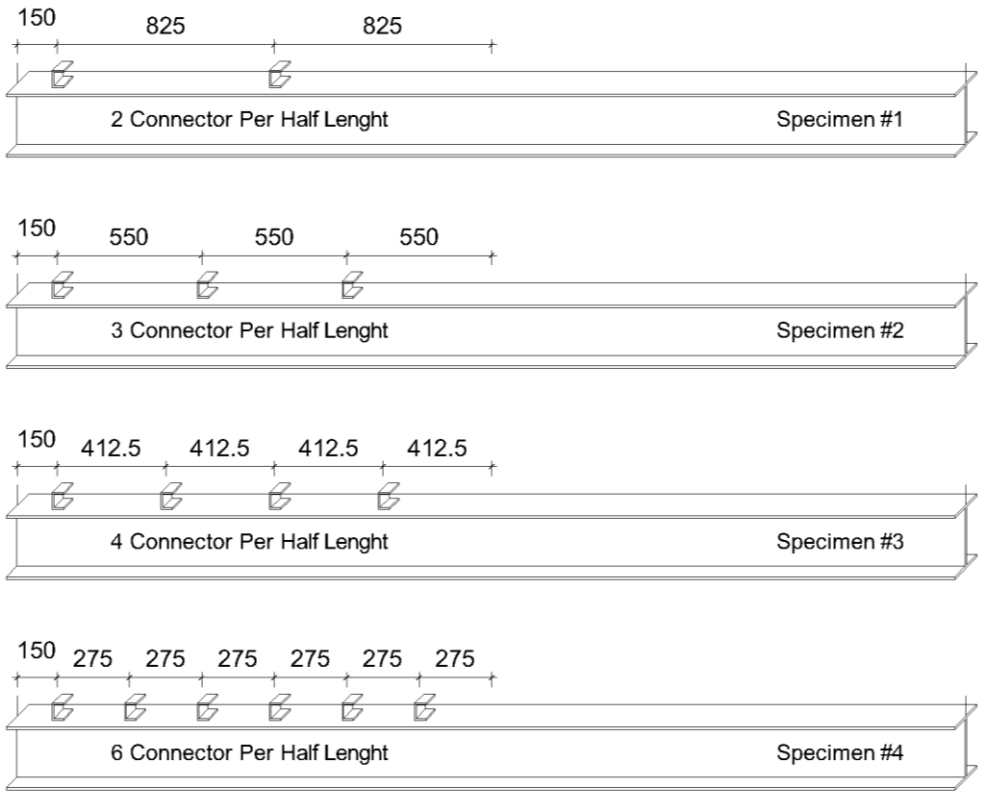

Figure 3.2 Full-Scale Beam Specimens (dimensions in mm)

These tests were part of a project that included the previous study done by Baran and Topkaya. After push-out tests researchers started working on full-scale beams with channel shear connectors. While this thesis was being written the research was in progress. Therefore this thesis contains only the four full-scale beam specimens and their test results.

3.3 Element Types

Element types used in modeling are summarized in Table 3.1.

Table 3.1 Element Types

Elements in Test Setup	Elements in ANSYS	Element Details
Steel Girder	SHELL181	4-Node Structural Shell
Concrete Deck	SOLID185	3D 8-Node Structural Solid
Channel Connectors	COMBIN39	Nonlinear Spring

The SHELL181 element was used to model the steel girder. This element is suitable for analysis of thin and moderately thick shell structures. SHELL181 is a four node element with six degrees of freedom at each node; translations in x, y and z directions and also rotations about x, y and z axes. Schematic drawing of the element is shown in Fig.3.3.

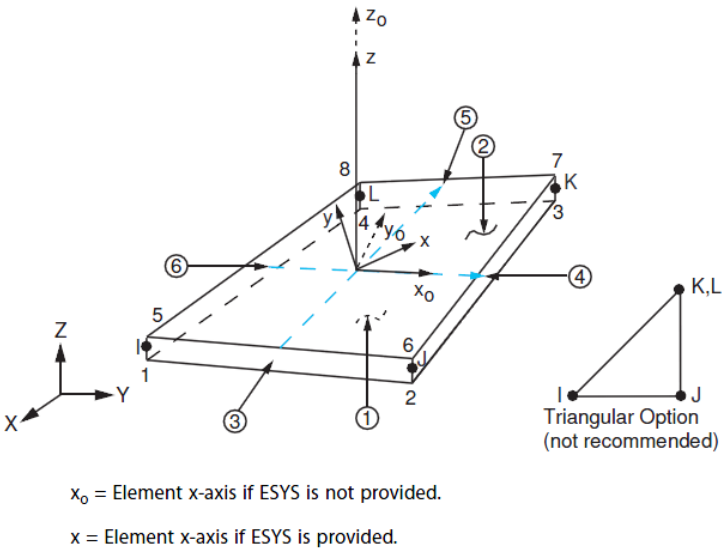

Figure 3.3 SHELL181 Geometry (Ref: ANSYS, 2010)

Thickness and layer information for the steel girder was set using section commands (SECDATA). To model the girder three sections were created without any layers, Bottom Flange, Web and Top Flange. Detailed modeling info is given in the following sections.

The SOLID185 element was used to model the concrete deck. This element is used for 3D modeling of the solid structures. The element has eight nodes with three degrees of freedom

at each node; translations in x, y and z directions. Also, SOLID185 has plasticity and large deflection capabilities. A schematic drawing for the element is shown in Fig.3.4.

The COMBIN39 element was used to model the behavior of the channel shear connectors. This approach simplifies the modeling. Instead of modeling the channel shear connectors as 3D objects COMBIN39 element mimics the load versus slip behavior of the connectors. COMBIN39 is a unidirectional element with nonlinear force-deflection capabilities. In all models it was used as a uniaxial tension-compression element with up to three degrees of freedom at each node; translations in x, y and z nodal directions. The schematic drawing of the element is shown in Fig.3.5.

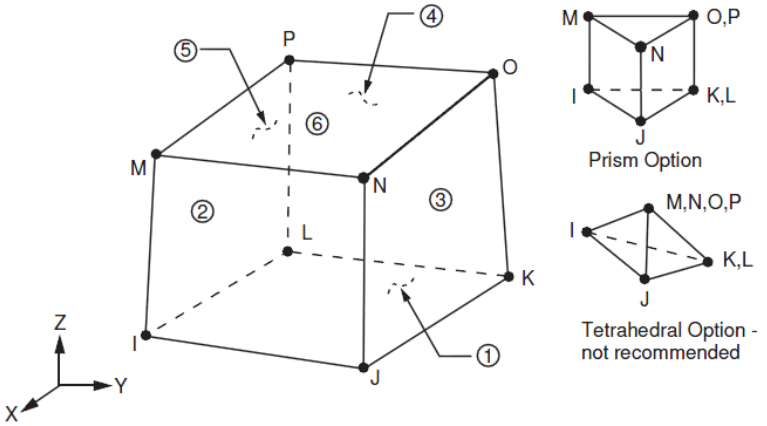

Figure 3.4 SOLID185 Geometry (Ref: ANSYS, 2010)

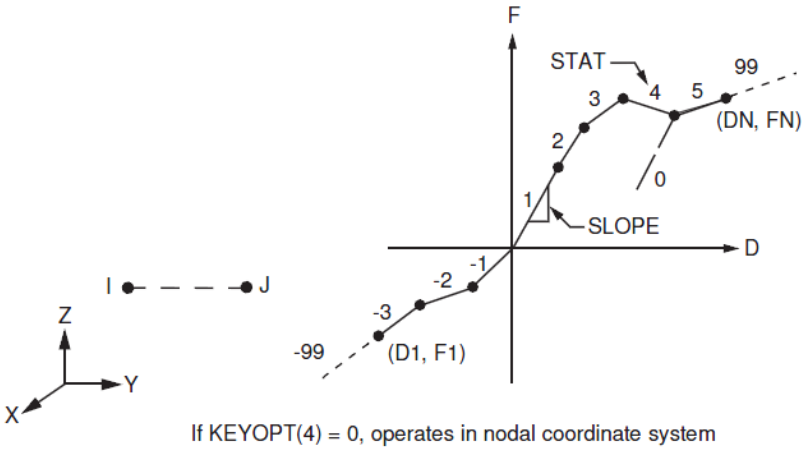

Figure 3.5 COMBIN39 Geometry (Ref: ANSYS, 2010)

Points on the curve (D_1, F_1, etc.) represent the force versus relative translation for the structural analyses. These data were set using real constants.

Further detailed information about the elements can be found in ANSYS User's Guides (ANSYS, 2010).

3.4 Real Constants

In ANSYS, real constants are used to specify properties of some elements. In this case, they were used to specify the force versus deflection behavior of the channel shear connectors. Instead of modeling the connectors they were simulated by nonlinear spring elements. To be able to do this, force versus deflection data was needed. As it was mentioned before in Chapter 1 and 2 there are load versus slip data from the push-out tests done by Baran and Topkaya (2012). Full-scale beam specimens were consisted of U65x50mm channel shear connectors so load vs. slip data of U65x50mm channel from push-out tests was used as real constants.

As it is mentioned in the modeling, because of the sectional symmetry channel connectors were modeled with half the capacity. It was assumed that the carried load was half the capacity but the slip was the same. According to that assumption U65-50mm load vs. slip data was modified as it is shown in Fig.3.6.

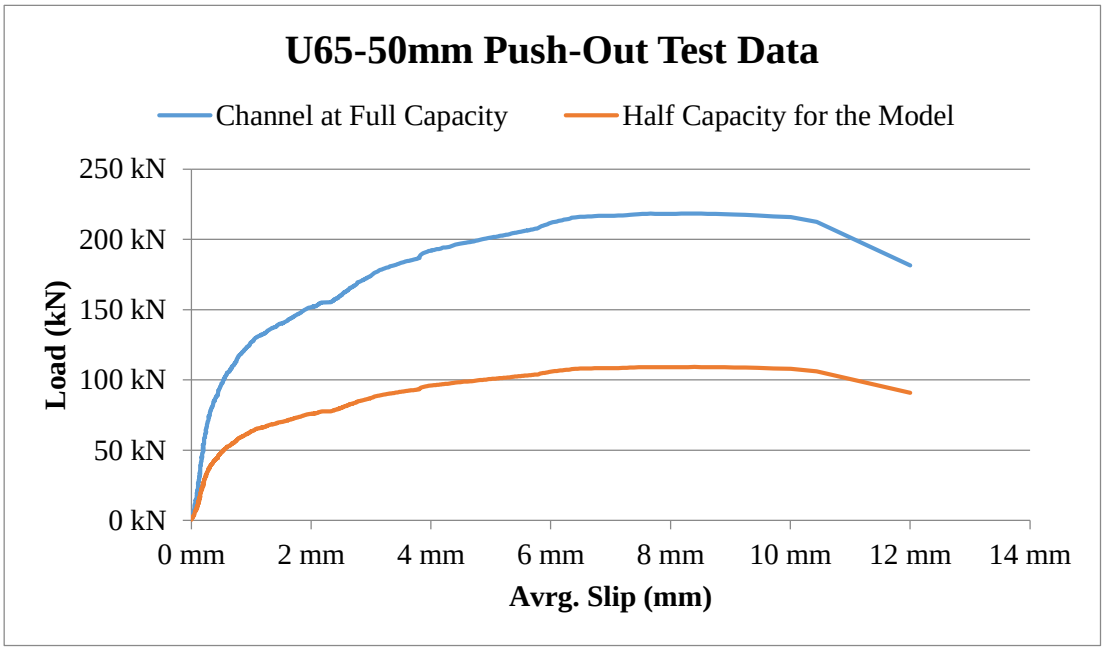

Figure 3.6 U65-50mm Channel Connector Push-Out Test Data

To define the behavior of the channel connector as in the push-out test, 20 data points that represents the best fit were taken from the given test results. Selected 20 points were presented in Table 3.2 and Fig.3.7.

These selected points were Real Constant Set 3, for COMBIN39 element. Note that every real constant set represents that individual element. No real constant set exists for other elements.

Table 3.2 Selected 20 Points for the COMBIN39

Points	Slip (mm)	Load (kN)	Points	Slip (mm)	Load (kN)
1	0.00 mm	0.00 kN	11	1.88 mm	74.74 kN
2	0.04 mm	3.61 kN	12	2.33 mm	77.68 kN
3	0.11 mm	11.12 kN	13	2.98 mm	86.71 kN
4	0.20 mm	24.59 kN	14	3.71 mm	92.74 kN
5	0.27 mm	34.62 kN	15	4.10 mm	96.50 kN
6	0.35 mm	40.58 kN	16	5.08 mm	100.92 kN
7	0.46 mm	46.58 kN	17	6.26 mm	107.17 kN
8	0.70 mm	55.05 kN	18	7.20 mm	108.52 kN
9	0.86 mm	59.97 kN	19	8.30 mm	109.17 kN
10	1.21 mm	66.38 kN	20	9.00 mm	109.17 kN

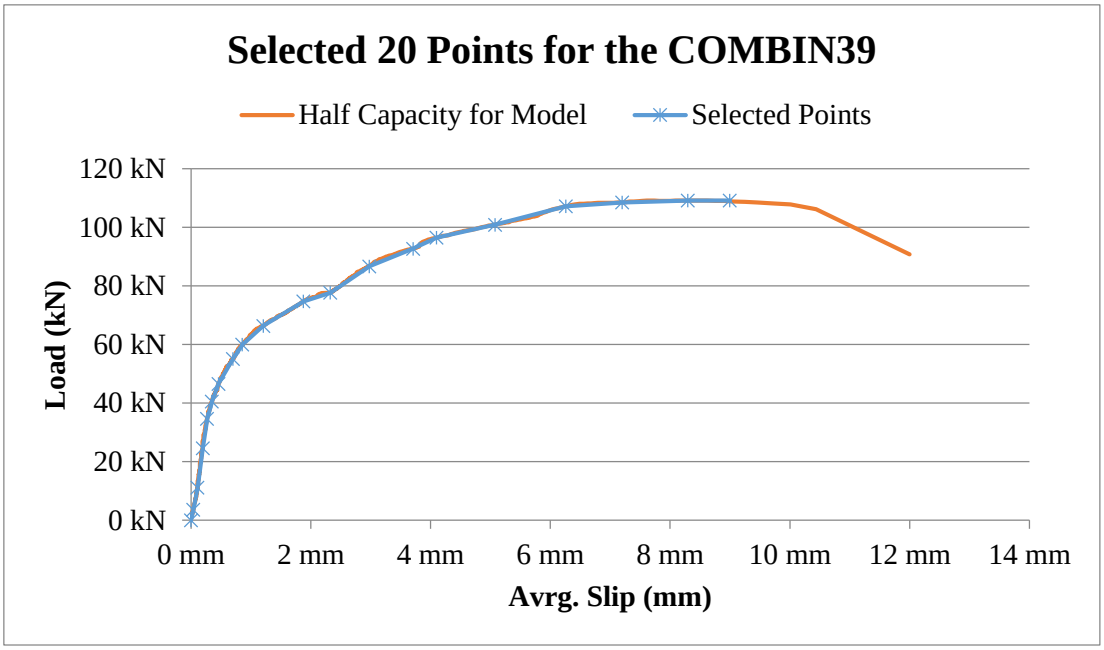

Figure 3.7 Selected 20 Points for the COMBIN39

3.5 Material Properties

There were three concrete modeling approaches tried in this thesis. One of them was the method mentioned in Kachlakev et al. (2001). The other two was mentioned in Wight and MacGregor (2009); Modified Hognestad and Todeschini methods.

Kachlakev et al. (2001)

Besides being widely used, this model includes concrete cracking and crushing and requires the SOLID65 element. The element requires linear isotropic and multilinear isotropic

material properties to properly model the concrete. The multilinear model uses von Mises failure criterion alongside the William and Warnke (1974) method to define concrete failure.

Implementation of the William and Warnke (1974) method to ANSYS (2010) requires nine different constants and those constants are;

1. Shear transfer coefficients for an open crack,
2. Shear transfer coefficients for a closed crack,
3. Uniaxial tensile cracking stress,
4. Uniaxial crushing stress (positive),
5. Biaxial crushing stress (positive),
6. Ambient hydrostatic stress state for use with constants 7 and 8,
7. Biaxial crushing stress (positive) under the ambient hydrostatic stress state (constant 6),
8. Uniaxial crushing stress (positive) under the ambient hydrostatic stress state (constant 6),
9. Stiffness multiplier for cracked tensile condition.

While the first four constants are definitive the other five were set to default.

Without getting into more detail this model was one of the tried methods however there were complications which made this model unusable. And those complications are addressed in the following sections.

Modified Hognestad (Wight and MacGregor, 2009)

This model is one of the common representations of the stress-strain curve for concretes with strengths up to 6000psi (41.4MPa). The stress-strain curve for the model is shown in Fig.3.8.

Model consists of a second degree parabola with the highest point at $1.8\,f_c''/E_c$ where $f_c'' = 0.9f_c'$ followed by a downward sloping line ending at a stress of $0.85f_c''$ with the limit strain of 0.0038. Formula for the parabola is;

$$f_c = f_c'' \left[2\left(\frac{\epsilon_c}{\epsilon_0}\right) - \left(\frac{\epsilon_c}{\epsilon_0}\right)^2 \right] \qquad \text{(Eq.3.1)}$$

The reduced strength $f_c'' = 0.9f_c'$ is for the difference between cylinder strength and the member strength.

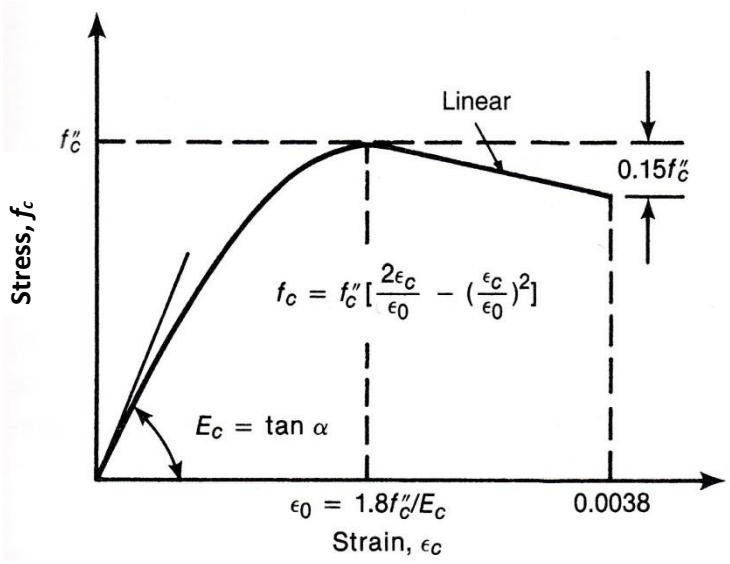

Figure 3.8 Stress-Strain Curve for Modified Hognestad

Todeschini (Wight and MacGregor, 2009)

This model is convenient for use in analytical studies including concrete strength up to 6000psi (41.4MPa) because the entire curve is represented by one function. The stress-strain curve for the model is given in Fig.3.9.

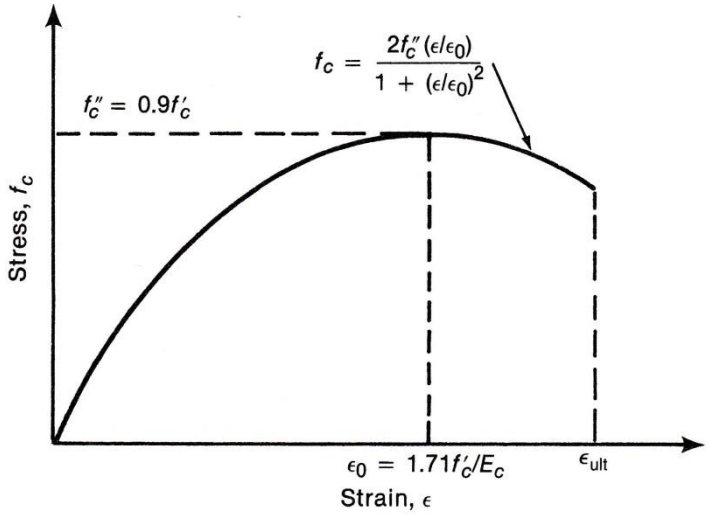

Figure 3.9 Stress-Strain Curve for Todeschini

The highest point on the curve, f_c'', is equal to $0.9f_c'$. The strain for the maximum stress is equal to $1.71\,f_c'/E_c$. For any given strain ϵ, $x = \epsilon/\varepsilon_0$ and the stress corresponding to that strain is;

$$f_c = (2f_c''.x)/(1+x^2) \qquad \text{(Eq.3.2)}$$

Between these three models Modified Hognestad method was found to be the most suitable for modeling the concrete slab. Comparisons between the models are shown in the Fig.3.10.

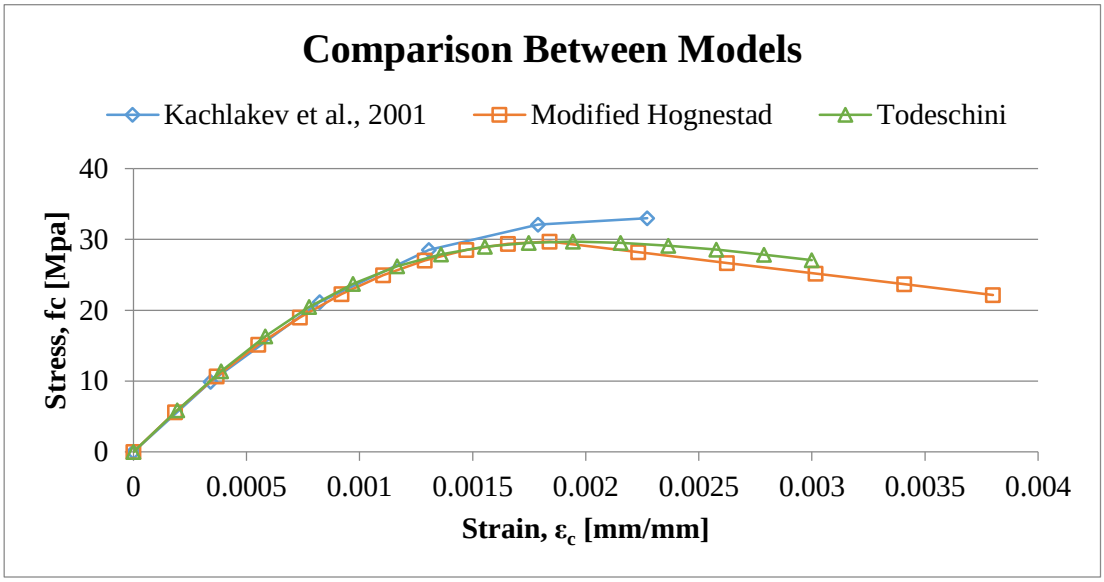

Figure 3.10 Comparison Between Concrete Material Models

Parameters needed to define the material models are listed in Table 3.3.

As it can be seen from the table both material models consist of two parts; linear and nonlinear. While steel girder was modeled as bilinear, concrete slab was modeled as multilinear using previously mentioned Modified Hognestad method.

Material Model 1 was used to model the steel girder connector. SHELL181 requires linear isotropic and bilinear kinematic properties to properly model the steel material. Bilinear material model is based on von Mises failure criteria. EX is the elasticity modulus of the channel connectors (E_s *: 200GPa*) and PRXY is the Poisson's ratio (ν *: 0.3*). Bilinear model also requires the yield strength (f_y) and the hardening modulus of the steel. The yield stress for all channel connectors was taken as 320MPa, and the hardening modulus was 2GPa as 1% of the elasticity modulus (Table 3.3).

Material Model 2 was used to model the concrete slab. SOLID185 element requires linear isotropic and multilinear kinematic (KINH) material properties to model concrete. The multilinear kinematic material uses the von Mises failure criteria as well as the Material Model 1. The elasticity modulus of the concrete (E_c) was calculated using the same equation in Chapter 2, Eq.2.1. For the multilinear kinematic properties fifteen points were selected from the Modified Hognestad model (Table 3.3).

Table 3.3 Material Models for the Analysis

Material Model	Element Type	Material Properties	
1	SHELL181	Linear Isotropic	
		EX :	200 GPa
		PRXY :	0.3
		Bilinear Kinematic	
		Yield Stress :	0.32 GPa
		Tang. Mod. :	2 GPa
2	SOLID185	Linear Isotropic	
		EX :	30.65 GPa
		PRXY :	0.2
		Multilinear Kinematic (KINH)	
		Strain (mm/mm)	Stress (GPa)
		0.0001841	0.005643
		0.0003681	0.010692
		0.0005522	0.015147
		0.0007363	0.019008
		0.0009204	0.022275
		0.0011044	0.024948
		0.0012885	0.027027
		0.0014726	0.028512
		0.0016566	0.029403
		0.0018407	0.029700
		0.0022326	0.028194
		0.0026244	0.026688
		0.0030163	0.025182
		0.0034081	0.023677
		0.0038000	0.022171

3.6 Modeling

As it can be seen from Fig.3.1, beams are symmetrical in cross-section and loading is symmetrical to the beam. Because of these reasons symmetry was utilize in FE modeling and only the quarter of the beam was modeled.

Since only the quarter of the beam was modeled, the new model was 1.8m long and the concrete slab was 40cm wide. The symmetry axes of the model coincided with the center of the cross-section for the beam. Also, due to this symmetry the web of the steel girder was modeled with half the thickness, so sections were created accordingly (Table 3.4).

Table 3.4 Section Properties of the Steel Girder

Sections of the Steel Girder	Section Number	Section Thickness	Element
Bottom Flange	1	tf	
Web	2	tw/2	SHELL181
Top Flange	3	tf	

At the beginning nodal points were defined by their x, y and z coordinates. Then, using these nodal points and employing the EN command elements were modeled. By using APDL programming language and defining the every single element with EN, meshing process was skipped and the whole beam model was created already meshed as it is shown in Fig.3.11.

First the steel girder and then the concrete deck was modeled. Afterwards shear connectors were modeled between the nodal points of the girder and deck. Placement of the shear connectors were done as it is shown in the guides provided earlier (Table 3.5).

Table 3.5 Specimens Used in the Experiments and Their Related Models

Specimens	Related Models
Specimen #1	Model #1
Specimen #2	Model #2
Specimen #3	Model #3
Specimen #4	Model #4
*Specimen #4	*Model #5

Additionally, element type number, material number and real constant set number for the models were set as shown in Table 3.6.

Table 3.6 Element Attributes for the Model

	Element Attributes		
Model Parts	Element Type	Material Number	Real Constant
Steel Girder	1	1	N/A
Concrete Deck	2	2	N/A
Channel Connector	3	N/A	3

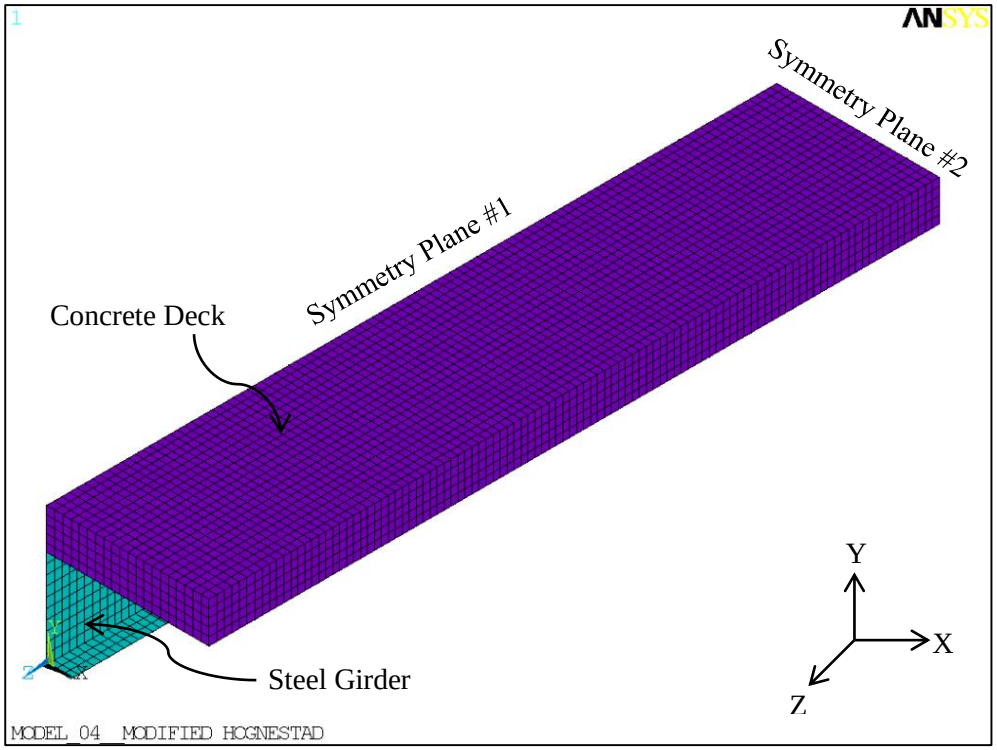

Figure 3.11 ANSYS Model

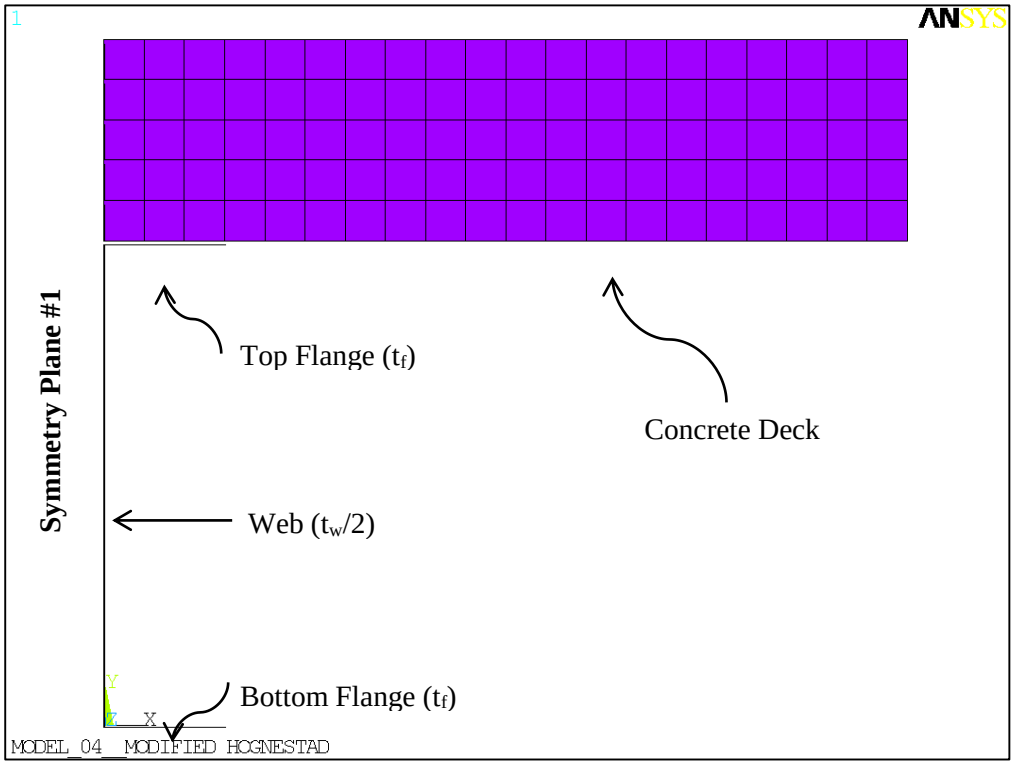

Figure 3.12 Cross-Section of the Beam Model

3.7 Loads and Boundary Conditions

Boundary conditions are needed to constraint the model to ensure that the model acts like beams in the experimental setup. For these models boundary conditions are;

- Coupled node sets
- Symmetry boundary conditions
- Support conditions.

For this setup, besides the shear connectors steel girder and concrete deck act together. Thus coupled node sets were employed to connect the two medium to act together. However, they were set to connect the mediums in only two directions x and y. This way shear connectors were set to work in only the z direction. Coupled sets are shown in Fig.3.13.

Symmetry planes were presented in Fig.3.11. For symmetry plane 1 (YZ plane), boundary conditions were set to constraint the beam for translations in x direction and rotations about y and z axes (Fig.3.13). Furthermore, for symmetry plane 2 (XY plane), constraints were set to prohibit translations in z direction and rotations about x and y axes (Fig.3.14).

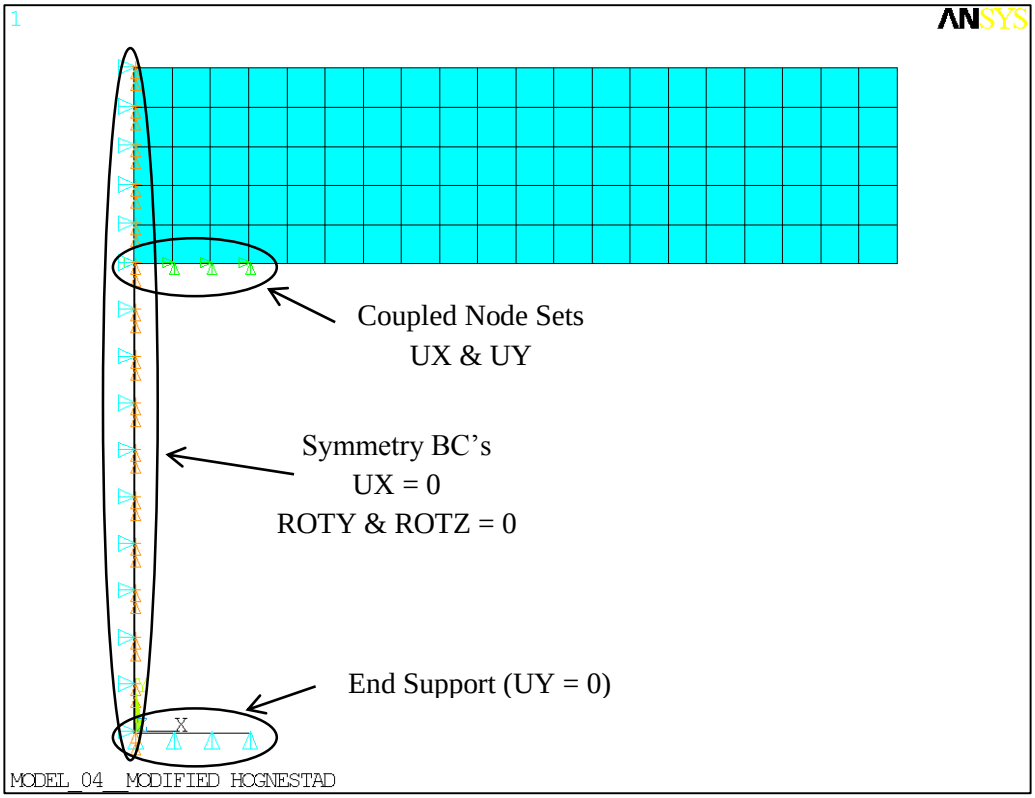

Figure 3.13 Boundary Conditions for the Model

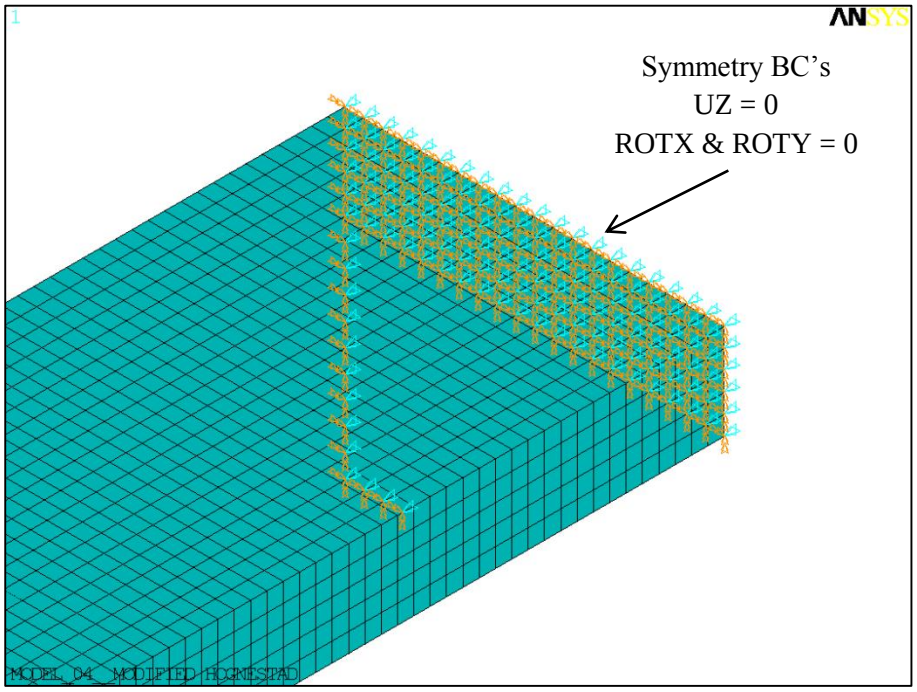

Figure 3.14 Boundary Conditions for Symmetry Plane #2

Beams in the experimental setup were simply supported. Because of that the closest end of the beam was constrained to prevent displacement in y direction. Only the bottom flange of the steel girder was constrained against movement. Support condition is shown in Fig.3.13.

In the experimental setup beams were loaded in the middle by a concentrated load. In the quarter model beams were loaded from their webs. The concentrated load was distributed along the web of the girder. Because of the symmetry by two planes when it comes to consider the results applied load was multiplied by four. Load application is shown in Fig.3.15.

As it was mentioned previously, there were four specimens in the test. However in the process of modeling one more alternative was created, one more model to represent the behavior of full composite action (Table 3.5).

This alternative fifth model was exactly the same model used for specimen number four however this did not included shear connectors. As it was depicted in the Fig.3.2 models included spring elements for channel shear connectors. Instead of using spring elements this time coupled node sets were employed. The nodes between concrete deck and steel girder were coupled in x, y and z directions. By this way girder and deck was connected to act as one.

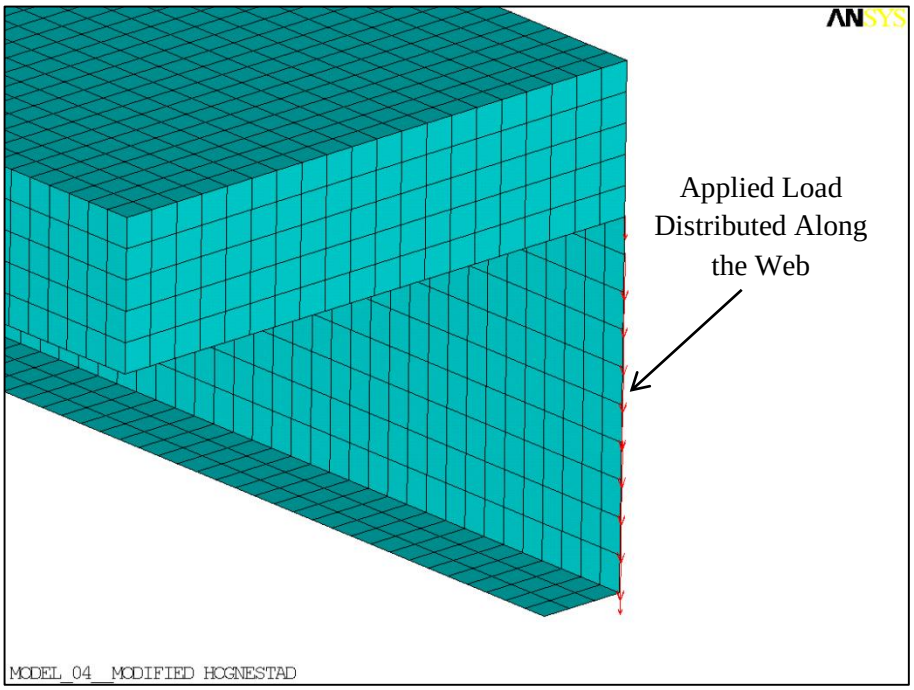

Figure 3.15 Load Application to the Beam

3.8 Analysis and Solution Control

In the experimental setup full-scale beams were simply supported and transversely loaded at their mid-spans. Therefore for all models, static analysis option was utilized.

For every analysis in ANSYS solution control commands control the linear and nonlinear solution options. In all models, the typical commands used for nonlinear static analysis were listed in Table 3.7.

Nonlinear geometry was not considered for the beams thus analysis was set as small displacement and static. Solution method was different from what was used in Chapter 2. This time Arc-Length method was employed. This method was used to eliminate convergence problems that might be caused by material nonlinearities and complex nonlinear elements. Also it was selected to control the solution termination criteria. With this method when mid-span deflection reaches to a specific limit solution terminates. Further technical details about this method and solution process can be found in ANSYS User's Guides (ANSYS, 2010). Some of the Arc-Length control commands used in models were listed in Table 3.8.

Other solution control commands that were not mentioned in here were set as program defaults. After the analysis program was set to terminate and exit the solution.

Table 3.7 Basic Sol'n Control Commands

Analysis Options	
Small Displacement Static	Yes
Calculate Prestress effects	No
Time Control	
Automatic Time Stepping	Arc-Length
Number of Substeps	1000
Write Items to Results File	
All Solution Items	Yes
Frequency	Write Every Substep

Table 3.8 Arc-Length Control Commands

Arc-Length Options	
Activate Arc-Length Method	Yes
Max. Multiplier	4
Arc-Length Termination	Terminate at UY Limit
Displacement Limit	140 mm

3.9 Model Verification

After creating them, models were tested against closed form solutions to verify that they were working properly. Slip at the interface for the spring elements were compared with the closed form solution presented by Viest et al. (1997).

Researchers presented a theory of incomplete interaction and it started with the visualization of force transfer in composite beam with partial shear connection. They separated the problem into its parts; steel girder and the concrete deck (Fig.1.1). After lengthy derivations slip for the uniformly distributed load q was obtained for a composite beam (Eq.3.3).

$$s(x) = \frac{q.h}{EI_{abs}.\alpha^3}\left[\frac{1-cosh(\alpha l)}{sinh(\alpha l)}\right]cosh(\alpha x) + sinh(\alpha x) + \frac{\alpha l}{2} - \alpha x \quad \text{(Eq.3.3)}$$

Also, upon derivation these were defined;

$$EA_{eq} = \frac{(EA)_T (EA)_B}{(EA)_T + (EA)_B} \quad \text{(Eq.3.4)}$$

$$EI_{abs} = (EI)_T + (EI)_B \quad \text{(Eq.3.5)}$$

$$EI_{full} = EI_{abs} + EI_{eq}.h^2 \quad \text{(Eq.3.6)}$$

$$\alpha^2 = \frac{k_s}{EA_{eq}} \frac{EI_{full}}{EI_{abs}} \quad \text{(Eq.3.7)}$$

where;
k_s : shear stiffness of a shear connector per unit length
$(EA)_T$: axial stiffness of concrete deck
$(EA)_B$: axial stiffness of steel girder
$(EI)_T$: flexural stiffness of concrete deck
$(EI)_B$: flexural stiffness of steel girder

Example Problem:

The following problem was solved using ANSYS v13.0. Then results from the analysis and closed form solution were compared.

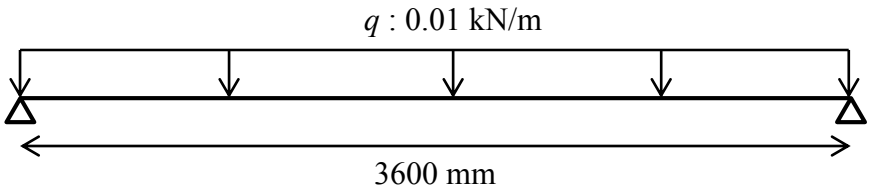

Figure 3.16.a Beam Dimension and Loading Information for Example Problem

Connector shear stiffness K_s=200 kN/mm and channels are spaced approximately 300mm from each other just like in specimen number four (Fig.3.2).

Calculations for closed form solution were made using MATLAB and a sample MATLAB code is given in Appendix A.

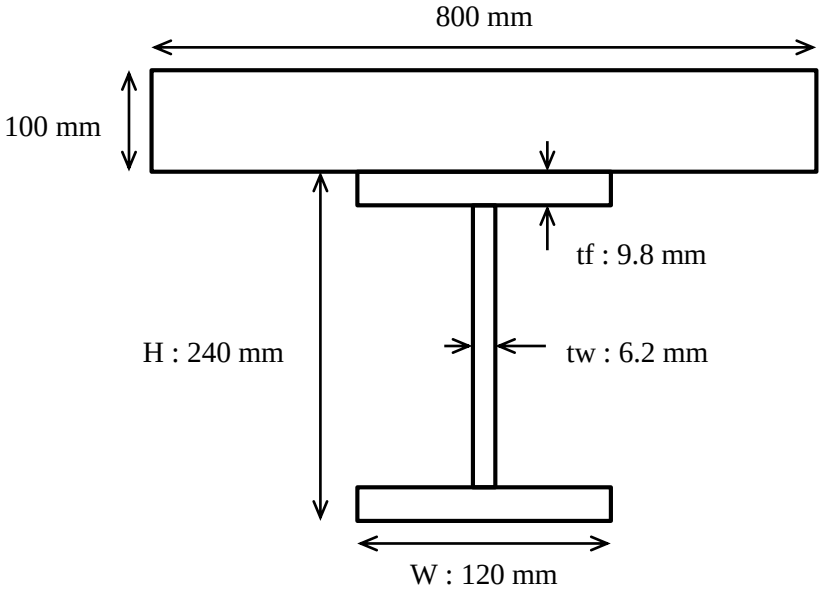

Figure 3.16.b Cross-Sectional Properties of the Beam for Example Problem

The results from Eq.3.3 and ANSYS were plotted in Fig.3.17. After that connector spacing was decreased to 100mm and calculations were repeated, the new plot can be found in Fig.3.18.

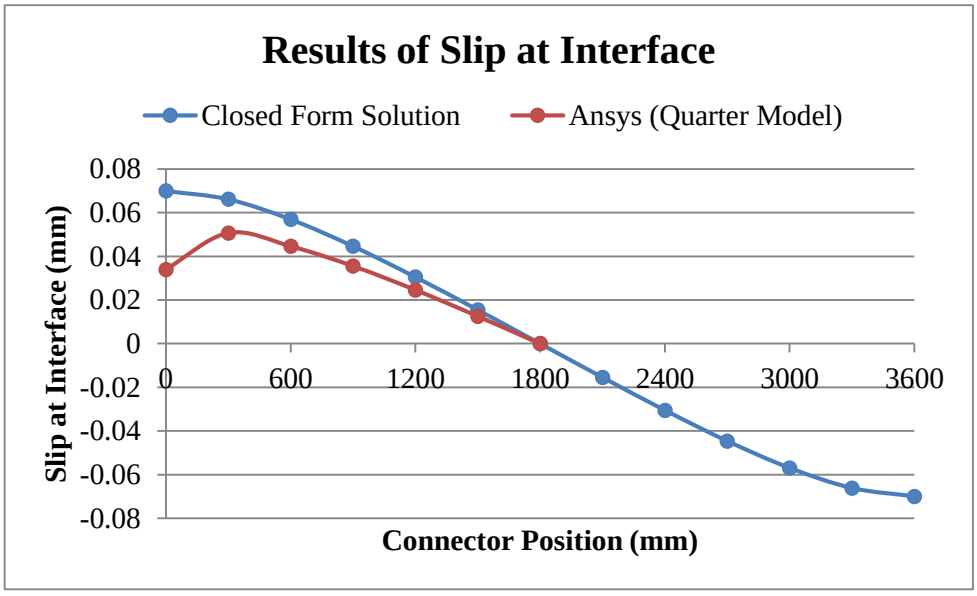

Figure 3.17 Results from Closed Form Solution and Ansys – Spacing : 300mm

As it can be seen from the Fig.3.17 and Fig.3.18 closed form solution and ANSYS slip results were in agreement.

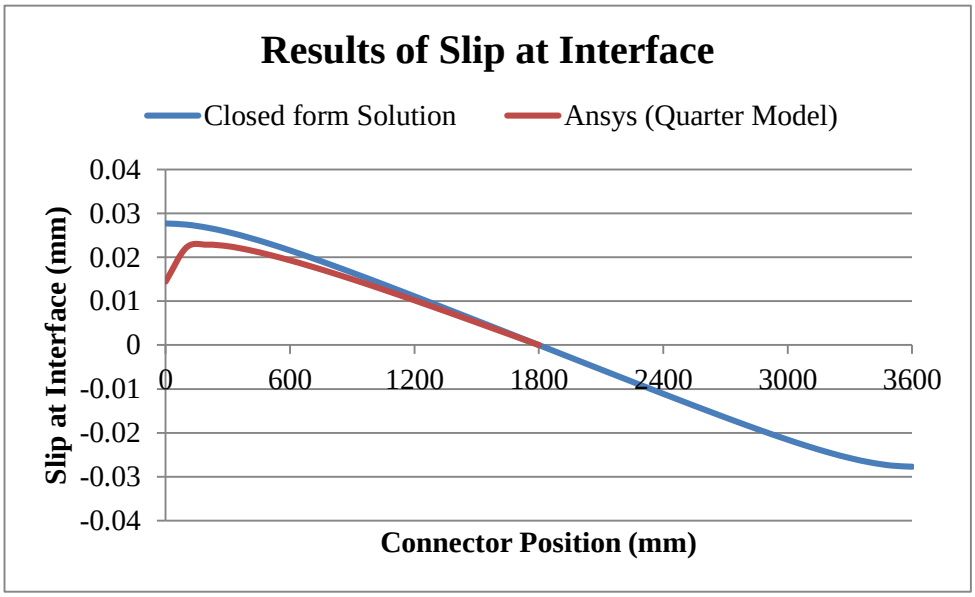

Figure 3.18 Results from Closed Form Solution and Ansys – Spacing : 100mm

Because of the symmetry ANSYS solution is half the length. Furthermore, even though analysis slip starts with slight difference it catches up quickly to the closed form solution.

3.10 Results

The primary goal of these models was to simulate the full-scale experiments done by Baran and Topkaya. However there were couple of aspects to these models;

- Several models with different concrete modeling approaches were generated. However, currently used approach was found to be the most stable and successful one.
- As a modeling strategy nonlinear spring elements were assigned as shear connectors. Thus the performances of these elements in their assigned roles were examined.
- Relationship between connector placement and partial to fully composite interaction was reviewed in 3D FE models.

Results from the analyses were compared with the load vs. midpoint deflection data collected during the experiments. A sample displaced shape is shown in Fig.3.19.

The next section includes comparisons and comments. Results from the models and the experiments are plotted in graphs to show the differences.

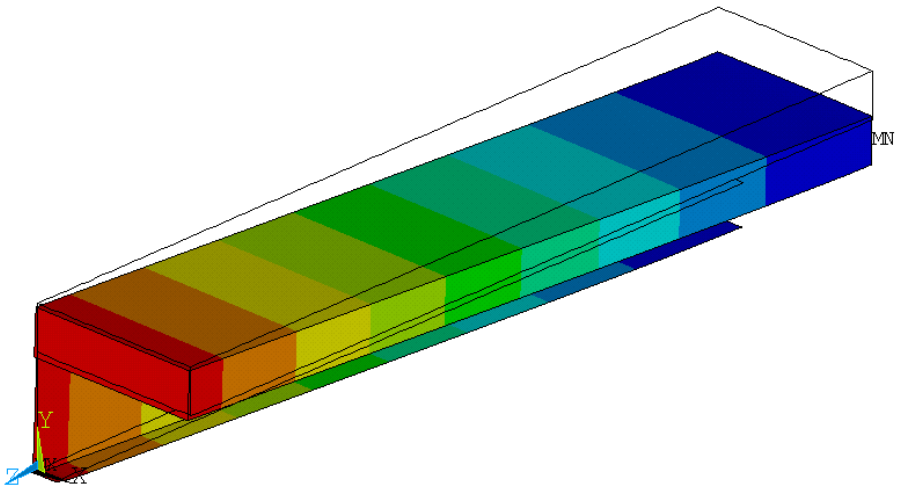

Figure 3.19 Deformed Shape of Model #4 (Contour Plot in UY)

3.11 Comparisons

This section compares and comments on the results of FE analyses. Results were given in the form of graphs and each includes the same aspects. To show the improvement in concrete modeling, results from an alternative model which includes steel and concrete as bilinear materials was added to the graphs. Thus every graph contains three cases; first the experimental results from an individual specimen collected during the full-scale beam tests, second the analysis results from that related model (Table 3.5) and third results from a model with bilinear materials.

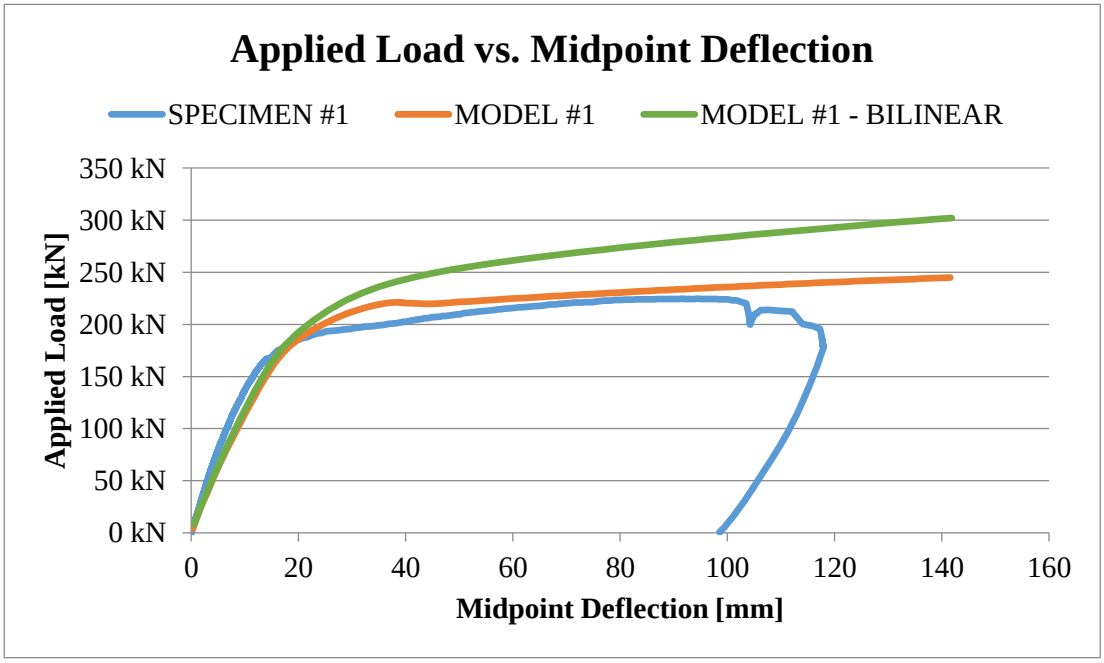

Figure 3.20 Applied Load vs. Midpoint Deflection Results of Specimen #1 & Model #1

As it can be seen from the Fig.3.20, initial stiffness of the specimen #1 and the model was quite close to each other. Also the capacity of the FE model is similar to the specimen. In 100mm deflection limit analysis results provide a 5.39 % capacity difference with experimental results. These results showed that the simulation of the specimen #1 was fairly successful.

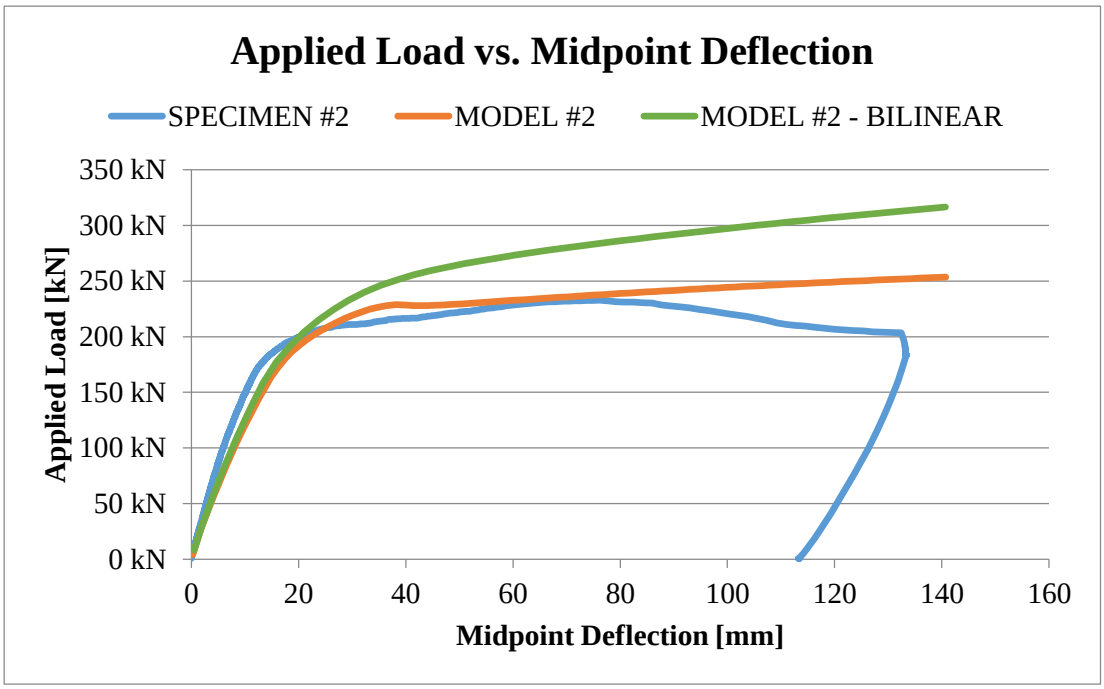

Figure 3.21 Applied Load vs. Midpoint Deflection Results of Specimen #2 & Model #2

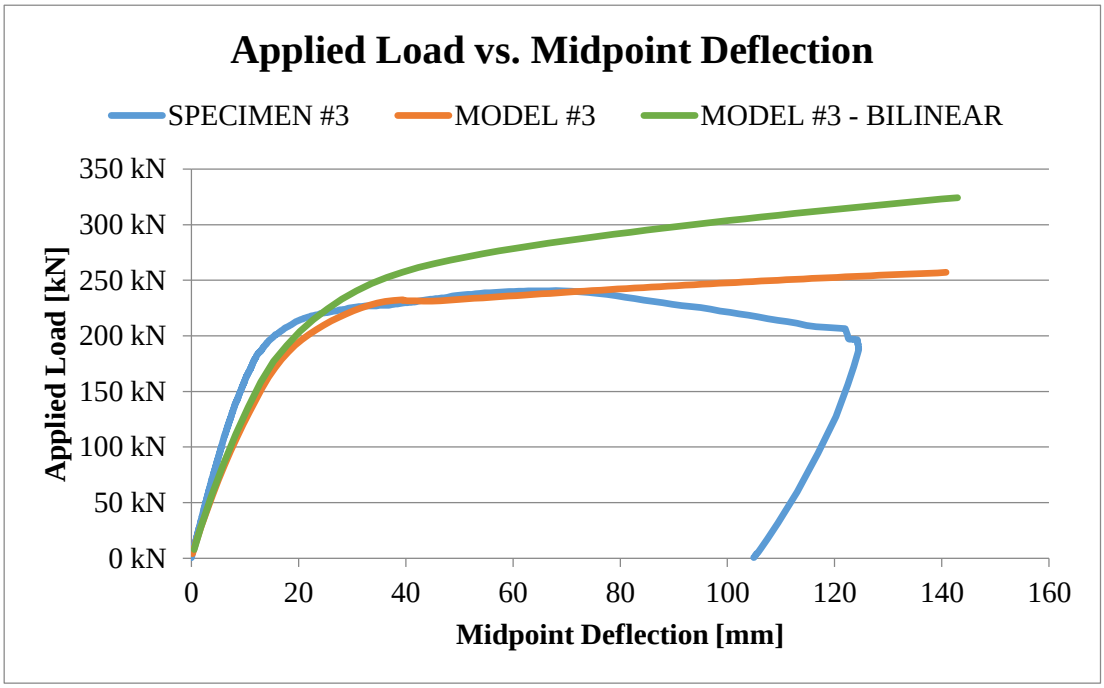

Figure 3.22 Applied Load vs. Midpoint Deflection Results of Specimen #3 & Model #3

Just like before Fig.3.21 showed a good correlation between experimental specimen #2 and the FE model #2. Both initial stiffness and the ultimate capacity was a good fit for this case. The ultimate capacity differed 2.87% from the experimental results for this case. However there was a slight difference between the initial stiffness of the specimen and the model. For this case the only difference from the model #1 was the connector density, this time there were 3 connectors spaced with 550mm.

Although in Fig.3.22, the difference between the initial stiffness of the specimen #3 and model #3 increased although, the ultimate capacity was close to the experimental result with 2.89% difference. It can clearly be seen from the figure that increased connector density, increased the ultimate capacity and the initial stiffness. However despite the increase in connector density the stiffness of the specimen was higher than the model.

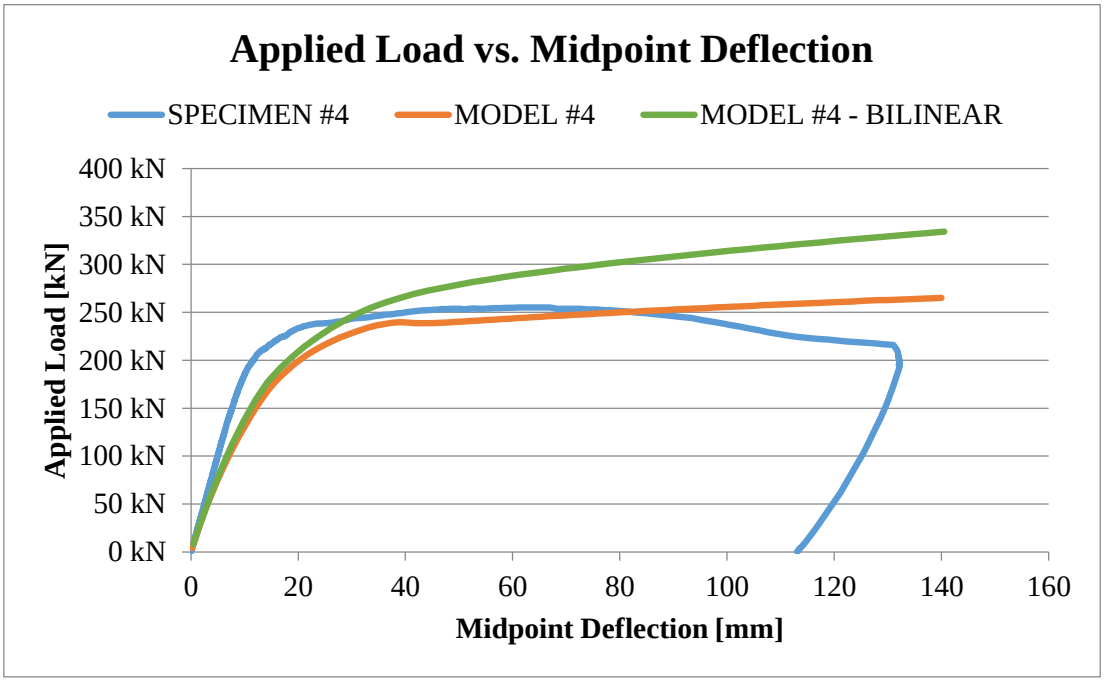

Figure 3.23 Applied Load vs. Midpoint Deflection Results of Specimen #4 & Model #4

Specimen #4 was the densest configuration and the Fig.3.23 showed that the difference between initial stiffness of specimen #4 and model #4 was not negligible. In FE model springs were not configured to work together even with the densest case. However, the ultimate capacity was the closes ever with 0.3%.

Through specimen number 1 to 4 connectors get denser and the initial stiffness differences increase between the models and the specimens. For this reason one alternative model was created (Model #5) to represent the full composite action.

Finally, the full composite action is shown in Fig.3.24. It can clearly be seen that the analysis model finally caught up with the specimens. Despite the higher ultimate capacity, model #5 showed the similar initial stiffness of the specimen #4. This means that the density in specimen #4 reaches the full composite action.

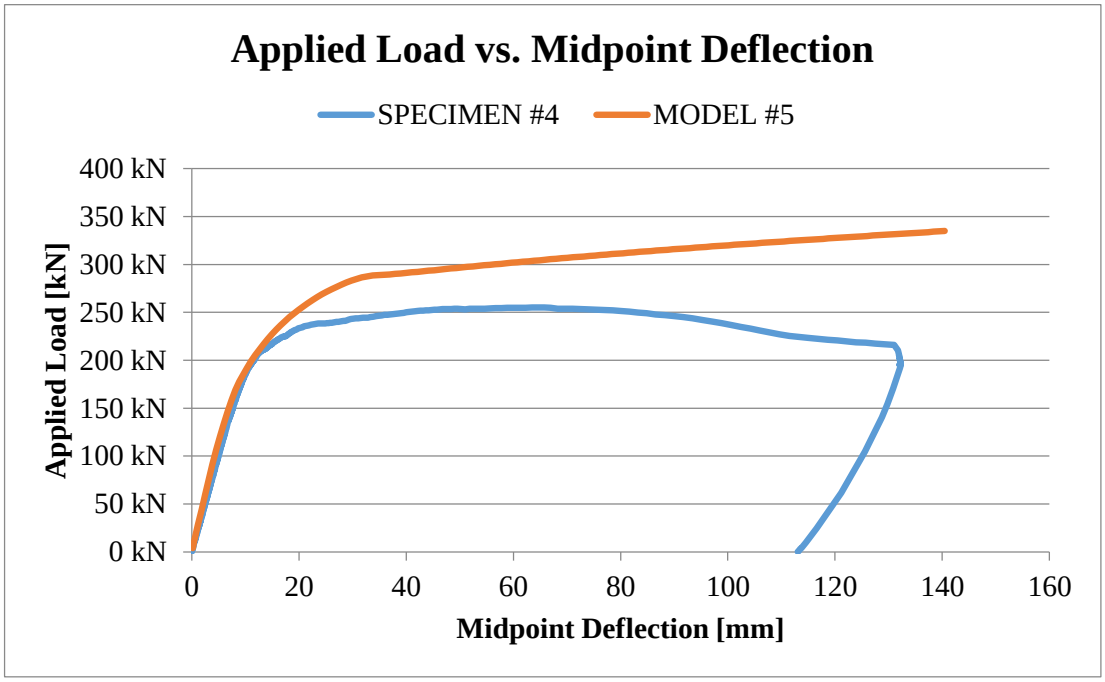

Figure 3.24 Applied Load vs. Midpoint Deflection Results of Specimen #4 & Model #5

The last figure showed that the spring modeling approach might need some improvements to reach the capacity of the specimens. Also, previous figures showed that even though changing concrete material modeling from bilinear to multilinear resulted in great improvements there was still room for improvements to be made.

In this current material modeling approach, concrete does not crack or crush thus the plateau and the descent in beam capacity did not happened. Due to that problem other concrete modeling techniques were tried.

Additionally, the slight difference in Fig.3.20 might be caused by difference in channel connector behavior. The representative behavior for the spring elements was taken from the push-out tests. There might be slight differences between specimens; the behavior of the channels in specimen #1 might perform slightly better than push-out test specimen U65-500mm. Because of that the difference in Fig.3.20 was negligible.

3.12 Other Concrete Modeling Approaches

To reach a better modeling for concrete element couple of different approaches was tried and these were;

- William and Warnke (1974) Failure Mode
- Drucker-Prager Model (ANSYS, 2010)
- Concrete Damage Model (ANSYS LS-DYNA, 2005)

William and Warnke (1974) Failure Mode

As it was mentioned before ANSYS supports concrete damage modeling with SOLID65 element. This material model with required element is capable of cracking and crushing. For cracking and crushing failures this model requires nine constants which four of them are definitive and the others can be calculated by program.

Two of these constants are empirical parameters and can change from one model to another. They are shear coefficient for open cracks and shear coefficient for closed cracks. There are several research papers that debate on these constants.

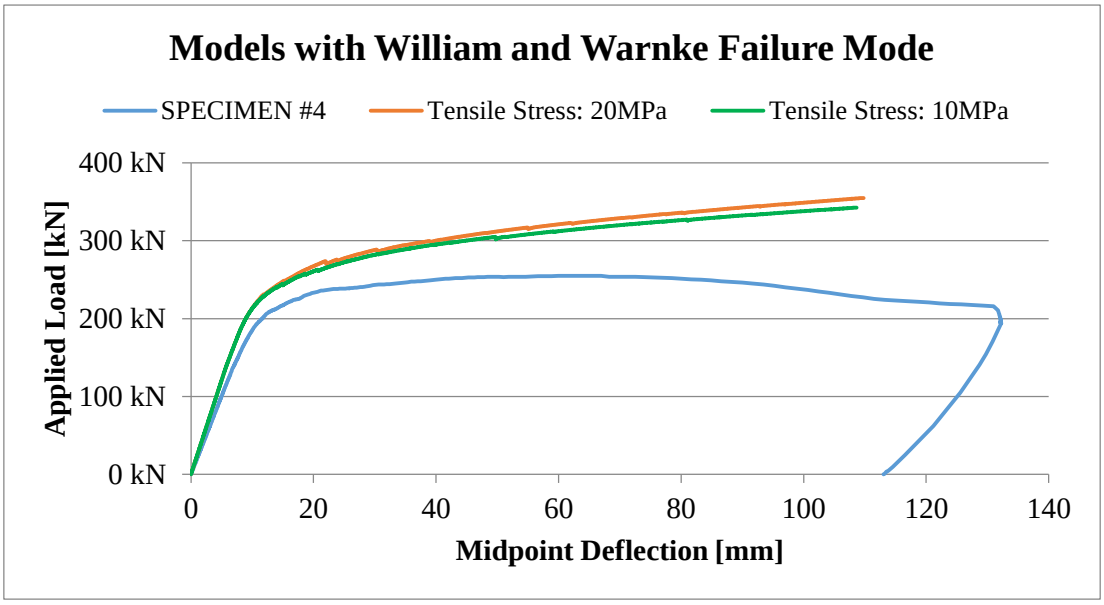

Figure 3.25 Results from Models with William and Warnke Failure Mode - 1

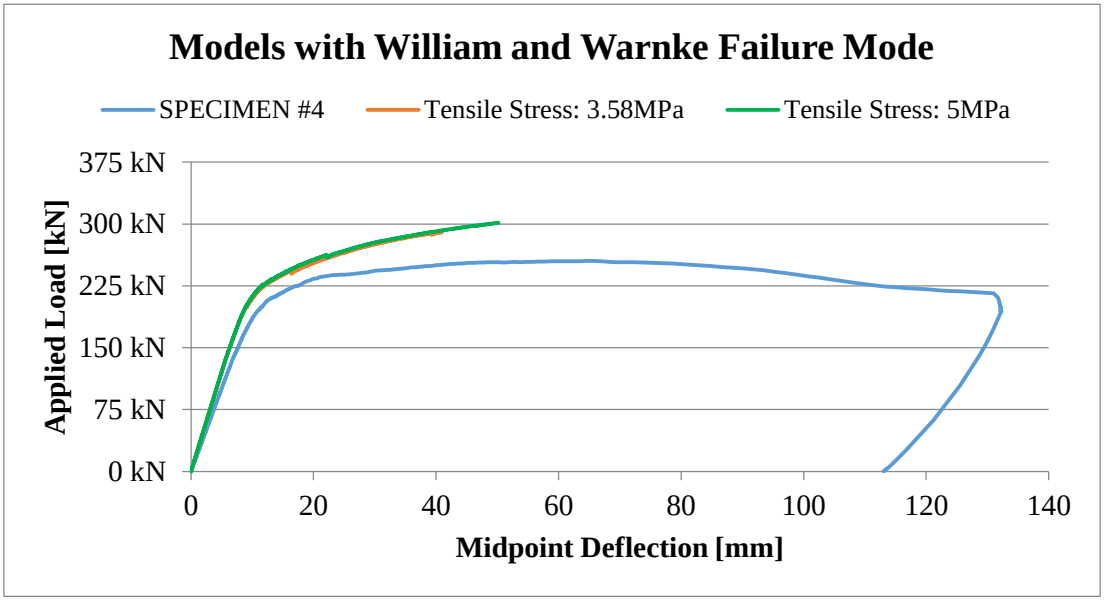

Figure 3.26 Results from Models with William and Warnke Failure Mode - 2

For the models in this thesis many coefficients were tried. However with crushing and cracking capabilities employed, solutions reached convergence problems every time. As a compromise crushing capabilities were turned off by setting uniaxial crushing stress as -1. Results showed that models with higher uniaxial tensile cracking stresses, such as 20 and 10MPa, reached conclusions without any convergence problems (Fig.3.25). However analysis of models with lower cracking stresses did not (Fig.3.26).

After couple of attempts because of the problems with convergence this model was abandoned.

Drucker-Prager Model (ANSYS, 2010)

After abandoning previous method, Drucker-Prager model was another alternative for concrete modeling. Generally this method was used for modeling granular materials such as soils, rock, and also concrete. This method uses the outer cone approximation to the Mohr-Coulomb law.

For this method three parameters were needed; c, cohesion, φ, angle of internal friction, and dilatancy angle.

After calculating these parameters, they were implemented to the model and solved. However despite several attempts convergence problems could not be averted and model was abandoned.

Concrete Damage Model (ANSYS LS-DYNA, 2005)

After all convergence problems, a trial model was generated using ANSYS LS-DYNA (2005). With the help of user's guides and research papers, Concrete Damage Model (ANSYS LS-DYNA, 2005) was found. To model a concrete in this approach, a great deal of material modeling experience was needed.

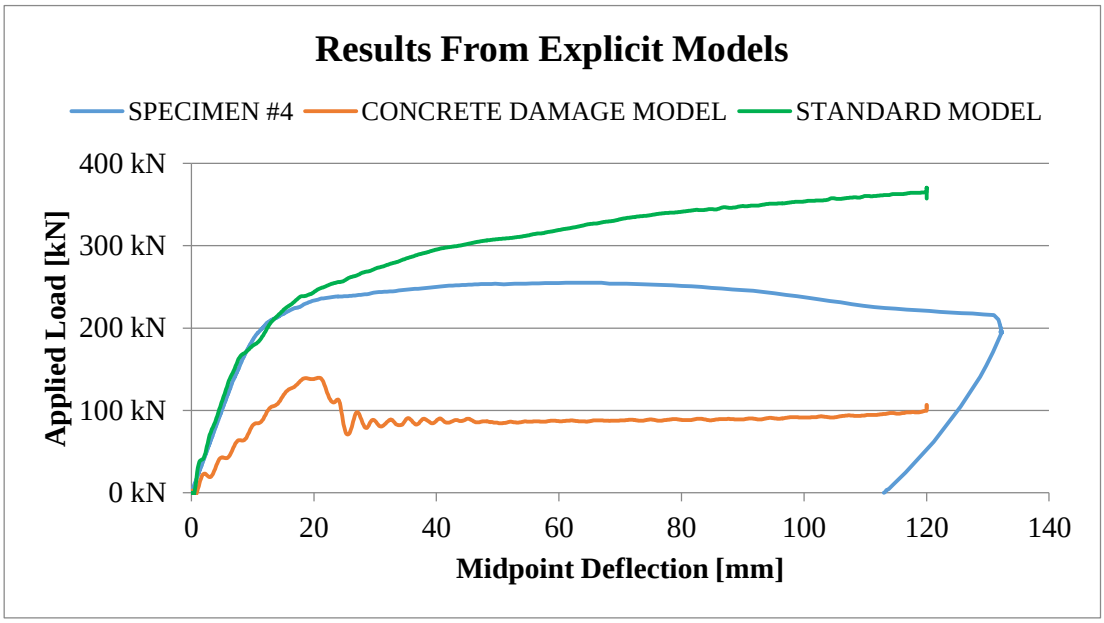

Figure 3.27 Results from Explicit Models

For accurate modeling 78 empirical parameters was required. Using the calculation technique in Malvar et al. (1997) and Wilt et al. (2011) all of the required parameters were calculated.

Despite the expectations concrete damage model revealed unsuccessful results (Fig. 3.27).

After abandoning the damage model, standard modeling technique was employed. However standard model resulted in nearly the same results from currently accepted concrete model with slightly higher capacity (Fig.3.27).

As a result, after trying all these modeling approaches this currently used multilinear kinematic model (Modified Hognestad) was the most stable and successful.

CHAPTER 4

SUMMARY, CONCLUSIONS AND FUTURE RECOMMANDATIONS

Even though shear studs are the most widely used shear connectors in composite beams, channel connectors present improvements and advantages over shear studs.

For many years, research focused on generating better formulas to predict the ultimate load capacity for channel shear connectors. However most of the research did not include the European sections and had problems with the equations. But with the study done by Baran and Topkaya (2012) a new inclusive formula was introduced in the result of a push-out test study with European channel sections as shear connectors.

In this thesis specimens from this study (Baran and Topkaya, 2012) were simulated using commercially available FE modeling program ANSYS v13.0. All ten specimens were modeled with simplistic 2D elements. Also steel channel and concrete deck were simulated using bilinear material models. Results from these analyses were compared with the results from the experiment and presented that even with simplistic FE models connector capacities can be predicted and results were quite sufficient.

After push-out tests, researchers continued to work on full-scale beam specimens with channel sections as shear connectors to investigate the partial and full composite action in composite beams.

In the light of that research, 3D full-scale beam models were created and several complex concrete modeling techniques were tried. Both explicit and implicit modeling approaches were tried but they failed to conclude in converged results. Although after many attempts one material model was found to be stable enough and selected for use. Results from this study were compared with results from full-scale beam experiments and showed that multilinear modeling provides even better results than bilinear modeling. Furthermore analysis results were sufficient enough to provide realistic beam capacities. Such as with the highest margin analysis results provide a 5.4% difference in ultimate capacity with 100mm deflection limit. However there are still improvements to be done.

As a recommendation to the future studies, more stable concrete modeling techniques can be integrated to the models. Also ways for including the concrete cracking and crushing properties to the FE models can be studied. Finally other available modeling programs can be employed for performance comparison.

REFERENCES

AISC, Specification for Structural Steel Buildings, American Institute of Steel Construction, Chicago, Illinois, 2005.

ANSYS, ANSYS User's Manual Release 13.0, ANSYS, Inc., Canonsburg, Pennsylvania, 2010.

ANSYS LS-DYNA, ANSYS LS-DYNA User's Guide Release 10.0, ANSYS, Inc., Canonsburg, Pennsylvania, 2005.

Baran, E., Topkaya, C., An Experimental Study on Channel Type Shear Connectors, Journal of Constructional Steel Research, Vol. 74, pp. 108-117, 2012.

CSA, Limit States Design of Steel Structures, CSA Standard CAN/CSA S16-01, Canadian Standards Association (CSA), Toronto, Ontario, 2001.

Chien, E.Y.L. and Ritchie, J.K., Design and Construction of Composite Floor Systems, Canadian Institue of Steel Construction, Toronto, Ontario, 1984.

Kachlakev, D.I., Miller, T., Yim, S., Chansawat, K., Potisuk, T., Finite Element Modeling of Reinforced Concrete Structures Strengthened With FRP Laminates, for Oregon Department of Transportation, SPR316, May, 2001.

Maleki, S. and Bagheri, S., Behavior of Channel Shear Connectors, Part I: Experimental Study, Journal of Constructional Steel Research, Vol. 64, pp. 1333-1340, 2008.

Maleki, S. and Bagheri, S., Behavior of Channel Shear Connectors, Part II: Analytical Study, Journal of Constructional Steel Research, Vol. 64, pp. 1333-1340, 2008.

Malvar, L.J., Crawford, J.E., Wesevich, J.W., Simons, D., A Plasticity Concrete Material Model for Dyna3D, International Journal of Impact Engineering, Vol. 19, Nos. 9-10, pp. 847-873, 1997.

Oehlers, D.J., Bradford, M.A., Composite Steel and Concrete Structural Members : Fundamental Behaviour, Pergamon, 1995.

Ollgaard, J.G., Slutter, R.G., and Fisher, J.W., Shear Strenght of Stud Connectors in Leightweight and Normal-Weigth Concrete, AISC Engineering Journal, Vol.8, pp. 55-64, April, 1971.

Pashan , A., Behaviour of Channel Shear Connctors: Push-Out Tests, M.Sc. Thesis, Department of Civil and Geological Engineering, University of Saskatchewan, Canada, 2006.

Siess, C.P., Composite Construction for I-Beam Bridges, Symposium on Highway Brigde Floors, Trans. ASCE, Vol. 114, pp. 1023-1045, 1949.

Siess, C.P., Viest, I.M., and Newmark, N.M., Studies of Slab and Beam Highways – Part III: Small-Scale Tests of Shear Connectors and Composite T-Beams, University of Illinois Bulletin No: 396,Urbana, IL., 1952.

Slutter, R.G., Driscoll, G.C., Flexural Strength of Steel-Concrete Composite Beams, Journal of the Structural Division, Proceedings of the American Society of Civil Engineers, Vol. 91, No. ST2, 1965.

Topkaya, C., Yura, J.A., and Williamson, E.B., Composite Shear Stud Strength at Early Concrete Ages, Journal of Structural Engineering, Vol. 6, pp. 952-960, 2004.

Viest, I.M., Colaco, J.P., Furlong, R.W., Griffis, L.G., Leon, R.T., and Wiley, L.A., Composite Construction Design for Buildings, ASCE Publications, McGraw-Hill, 1997.

Viest, I.M., Siess, C.P., Appleton, J.H., and Newmark, N.M., Full-Scale Tests of Channel Shear Connectors and Composite T-Beams, University of Illinois Bulletin No: 405,Urbana, IL., 1952.

Wight, J.K., MacGregor, J.G., Reinforced Concrete: Mechanics & Design, Fifth Edition, Pearson International Edition, Prentice-Hall, Inc., 2009.

William, K.J., Warnke, E.P., Constitutive Model for the Triaxial Behavior of Concrete, Seminar on Concrete Structures Subjected to Triaxial Stresses, International Association of Bridge and Structural Engineering Conference, Bergamo, Italy, pp.174, 1974.

Wilt, T., Chowdhury, A., Cox, P.A., Response of Reinforced Concrete Structures to Aircraft Crash Impact, for U.S. Nuclear Regulatory Commission Contract NRC−02−07−006, 2011.

APPENDIX A

MATLAB CODE FOR EXAMPLE PROBLEM

```
% Dimensions for Steel Girder
d_steel = 240;                  % height of the girder (mm)
tw_steel = 6.2;                 % web thickness of the girder (mm)
bf_steel = 120;                 % flange width of the girder (mm)
tf_steel = 9.8;                 % flange thickness of the girder (mm)
h_steel = d_steel-2*tf_steel;   % web height of the girder (mm)
% Properties of Steel Girder
Es = 200;                       % Elasticity Mod. of steel (GPa)
As = (h_steel*tw_steel)+2*(tf_steel*bf_steel);              % (mm^2)
Is = (h_steel^3*tw_steel/12)+2*(tf_steel^3*bf_steel/12)...
    +2*(tf_steel*bf_steel*(d_steel/2-tf_steel/2)^2);        % (mm^4)
% Dimensions for Concrete Deck
t_deck = 100;                       % thickness of the conc. deck (mm)
w_deck = 800;                       % width of the conc. deck (mm)
h = (d_steel/2+t_deck/2);           % distance between centroids (mm)
% Properties of Conc. Deck
Ec = 30.65;                         % Elasticity Mod. of conc. (GPa)
Ac = (t_deck*w_deck);                                   % (mm^2)
Ic = (t_deck^3*w_deck/12);                              % (mm^4)
% Parameters
EA_T = (Ec*Ac);                                         % (kN)
EA_B = (Es*As);                                         % (kN)
EI_T = (Ec*Ic);                                         % (kN.mm^2)
EI_B = (Es*Is);                                         % (kN.mm^2)
EA_eq = (EA_T*EA_B)/(EA_T+EA_B);                        % (kN)
EI_abs = (EI_T+EI_B);                                   % (kN.mm^2)
EI_full = EI_abs+EA_eq*h^2;                             % (kN.mm^2)
Ks = 200;                                               % (kN/mm)
spacing = 300;                                          % (mm)
ks = Ks/spacing;                                        % (kN/mm^2)
a_2 = (ks*EI_full)/(EA_eq*EI_abs);                      % (1/mm^2)
a = sqrt(a_2);                                          % (1/mm)
q = 0.01;                                               % (kN/mm)
L = 3600;                                               % (mm)
x = (0:spacing:L);                                      % (mm)
% Closed Form Solution & Plot
sx = ((q*h)/(EI_abs*a^3))*(((1-cosh(a*L))/sinh(a*L))*cosh(a.*x)...
    +sinh(a.*x)+a*L/2-a.*x);                            % (mm)
plot(x,sx)
% Write to .txt file
result = [x; sx];
fileID = fopen('new_slip_kt_1e2.txt','w');
fprintf(fileID,'%12s %20s\r\n','x','s(x)');
fprintf(fileID,'%12d %20.6E\r\n',result);
fclose(fileID);
```